Quarkonium production in pp and p-A collisions with ALICE at the LHC

Astrid Morreale in behalf of the ALICE collaboration
SUBATECH/CNRS
SQM – July 13 2017

Motivation

Quarkonia (J/ψ, $\psi(2S)$, Υ) proceed from the production of a heavy quark pair (either c or b) in a hard-scattering process.
This is followed by the evolution of the pair into a colorless bound state.

The heavy quark mass provides a high enough hard scale for pQCD to be applicable, however the evolution into a bound state is intrinsically non perturbative

What can we learn from measuring quarkonium production:

- pp: understand production mechanisms, probe PDFs, (particularly gluon's PDF's down to low *x)* , provide a reference to p-Pb and Pb-Pb measurements
- p-Pb: probe cold nuclear matter effects (i.e. modification of the PDFs, saturation, Cronin enhancement…)
- Pb-Pb: probe the formation and properties of the QGP (color screening, dissociation, recombination..)

Motivation

Quarkonia (**J/ψ, ψ(2S)**, ϒ) proceed from the production of a heavy quark pair (either c or b) in a hard-scattering process.
This is followed by the evolution of the pair into a colorless bound state.

The heavy quark mass provides a high enough hard scale for pQCD to be applicable, however, the evolution into a bound state is intrinsically non perturbative

What can we learn from measuring quarkonium production:

- **pp: understand production mechanisms, probe PDFs, (particularly gluon's PDF's down to low *x)* , provide a reference to p-Pb and Pb-Pb measurements**
- **p-Pb: probe cold nuclear matter effects (i.e. modification of the PDFs, saturation, Cronin enhancement…)**
- Pb-Pb: probe the formation and properties of the QGP (color screening, dissociation, recombination..)

Motivation

$$d\sigma^{Q} = f_a(x_a)\, f_b(x_b) \times d\hat{\sigma}_{ab}^{q\bar{q}} \times \left\langle O_{q\bar{q}}^{Q} \right\rangle$$

Quarkonium production cross section has three components

- parton distribution functions: describe the partonic (quark/gluons) content of the proton (soft scale, measured in e.g. DIS experiments)
- partonic cross section: describe how to produce the heavy quark pair from two partons (hard scale, short distances, calculable with pQCD)
- evolution of the heavy quark pair into the quarkonium state Q
  (soft scale, large distances and model dependent)

Motivation

$$d\sigma^{Q} = f_a(x_a)\, f_b(x_b) \times d\hat{\sigma}_{ab}^{q\bar{q}} \times \left\langle O_{q\bar{q}}^{Q} \right\rangle$$

Quarkonium production cross section has three components

- parton distribution functions: describe the partonic (quark/gluons) content of the proton (soft scale, measured in e.g. DIS experiments)
- partonic cross section: describe how to produce the heavy quark pair from two partons (hard scale, short distances, calculable with pQCD)
- evolution of the heavy quark pair into the quarkonium state Q (soft scale, large distances and model dependent)

Applicable to direct production.

When we measure inclusive quarkonia we have contributions from:

- decay from higher mass resonances (for J/ψ, they are the ψ(2S) and χ_c)
- decay from b-hadrons (non-prompt J/ψ, ψ(2S))

Outline

Recent **pp** RUN2 results at ALICE:

- J/ψ and ψ(2S) production at $\sqrt{s}$= 13 TeV and at forward rapidity
- Energy dependence of J/ψ and ψ(2S) production at forward rapidity

Recent **p-Pb** RUN2 results at ALICE:

- J/ψ production at $\sqrt{s_{NN}}$= 8.16 TeV and forward rapidity

More results in these systems as a function of multiplicity will be given in Ionut's talk following this presentation.

Forward-*y* charmonium measurements in ALICE

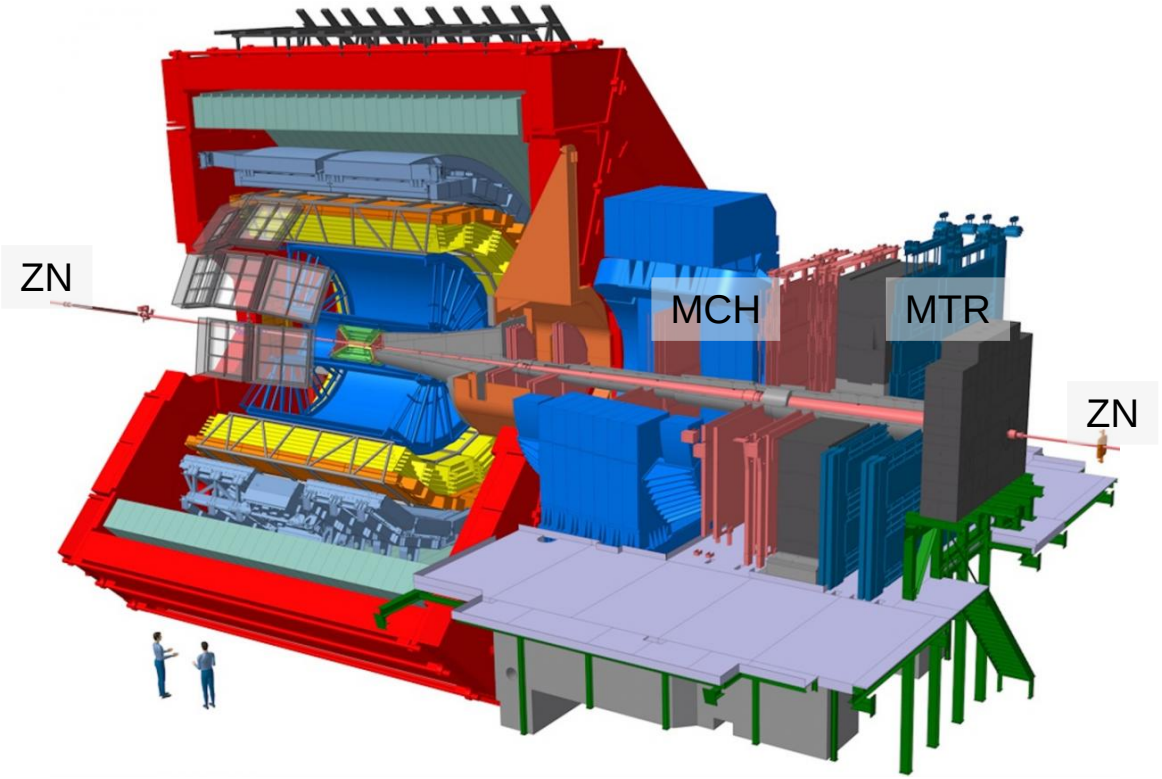

ALICE Muon system:

- 5 stations of tracking chambers (-4<η<-2.5)
- 2 stations of trigger chambers
- dipole magnet
- absorbers

Charmonia are measured in the μ+μ- decay channel, at forward rapidity (2.5<*y*<4) and down to p_T = 0 using

- ITS for vertex determination
- MTR for triggering
- MCH for tracking

V0 detectors are also used for triggering (in coincidence with MTR)
T0 detectors for luminosity determination
V0 and ZDC detectors are used for centrality determination in p-Pb

J/ψ and ψ(2S) production in **pp** collisions.

- J/ψ and ψ(2S) production at √s= 13 TeV and at forward rapidity
- Energy dependence of J/ψ and ψ(2S) production at forward rapidity

Data analysis

Quarkonia are measured using fits to the invariant mass distribution of $\mu^+\mu^-$ pairs detected in the muon system at forward rapidity

pp@13 TeV data sample from 2015 run at LHC

$$L_{int} = 3.2\ pb^{-1} \pm 3.4\%$$

Corresponds to: $N_{J/\psi} \sim 330k$

$N_{\psi(2S)} \sim 8k$

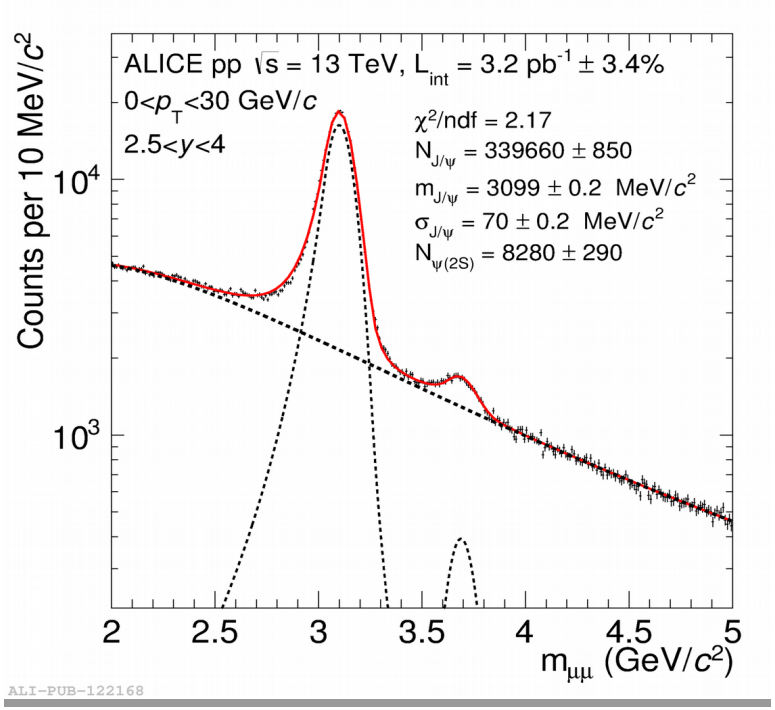

Eur. Phys. J. C 77 (2017) 392

Inclusive J/ψ and ψ(2S) at √s = 13 TeV

inclusive J/ψ

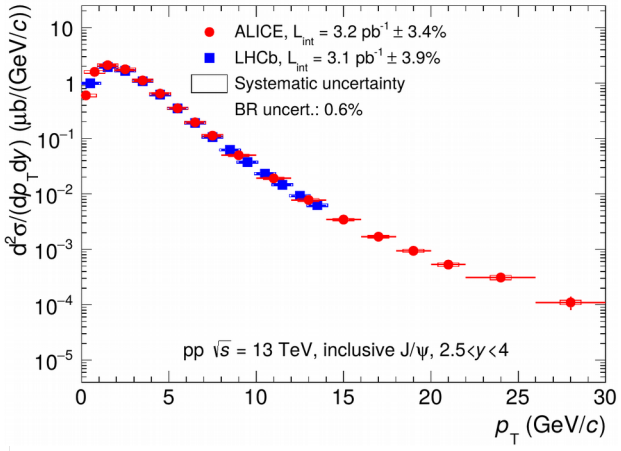

inclusive ψ(2S)

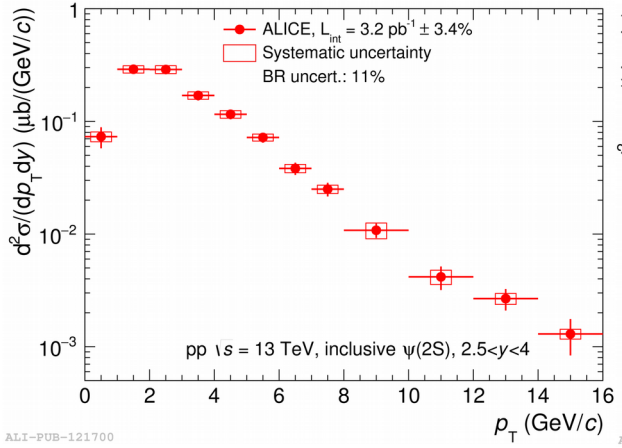

ψ(2S)-to-J/ψ ratio

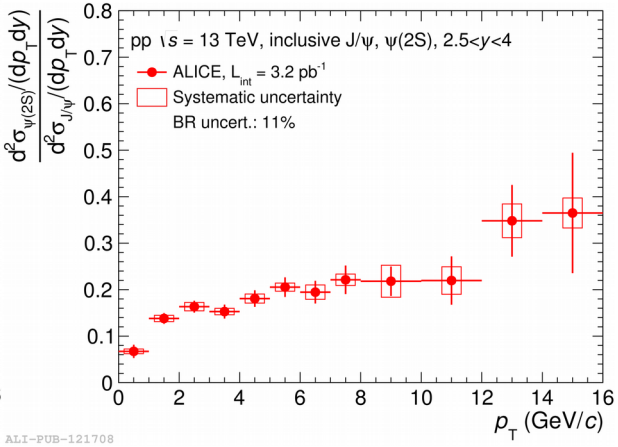

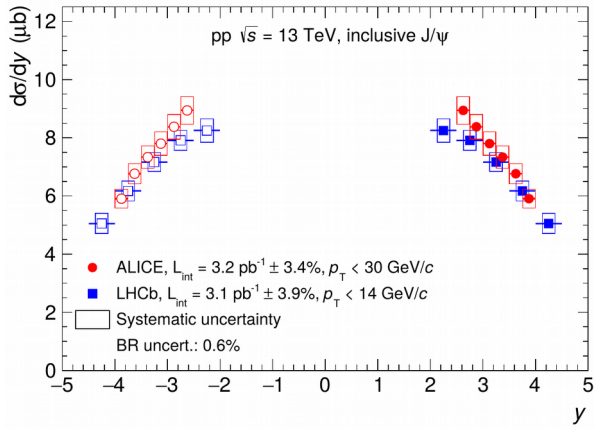

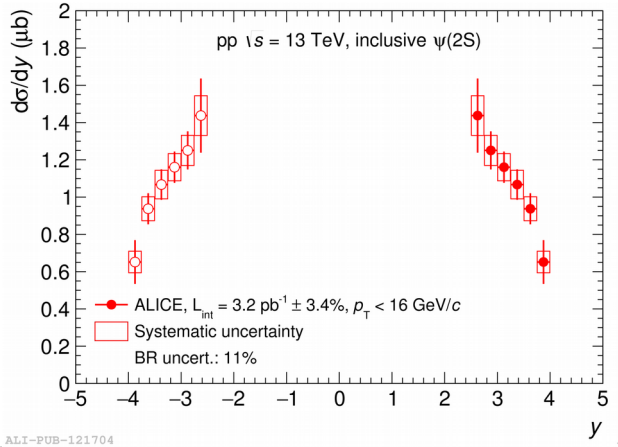

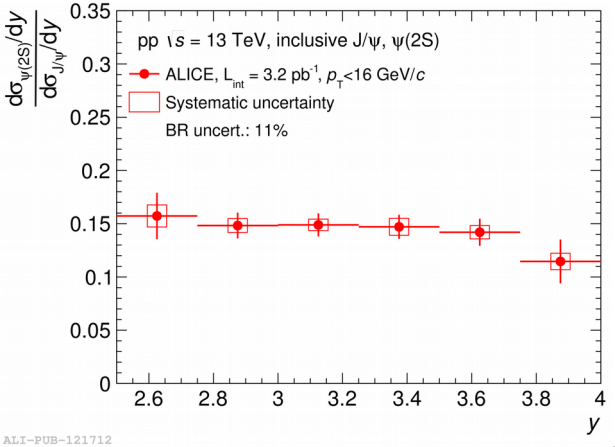

Left: Comparison to LHCb results (JHEP10 (2015) 172 and erratum)

LHCb quoted values correspond to the sum of the prompt and non-prompt contributions, integrated over the same rapidity range as ALICE (2.5<y<4)

ψ(2S): ALICE is the only measurement available at $\sqrt{s}$ =13 TeV down to p_T =0

Comparison to lower energy: J/ψ vs p_T

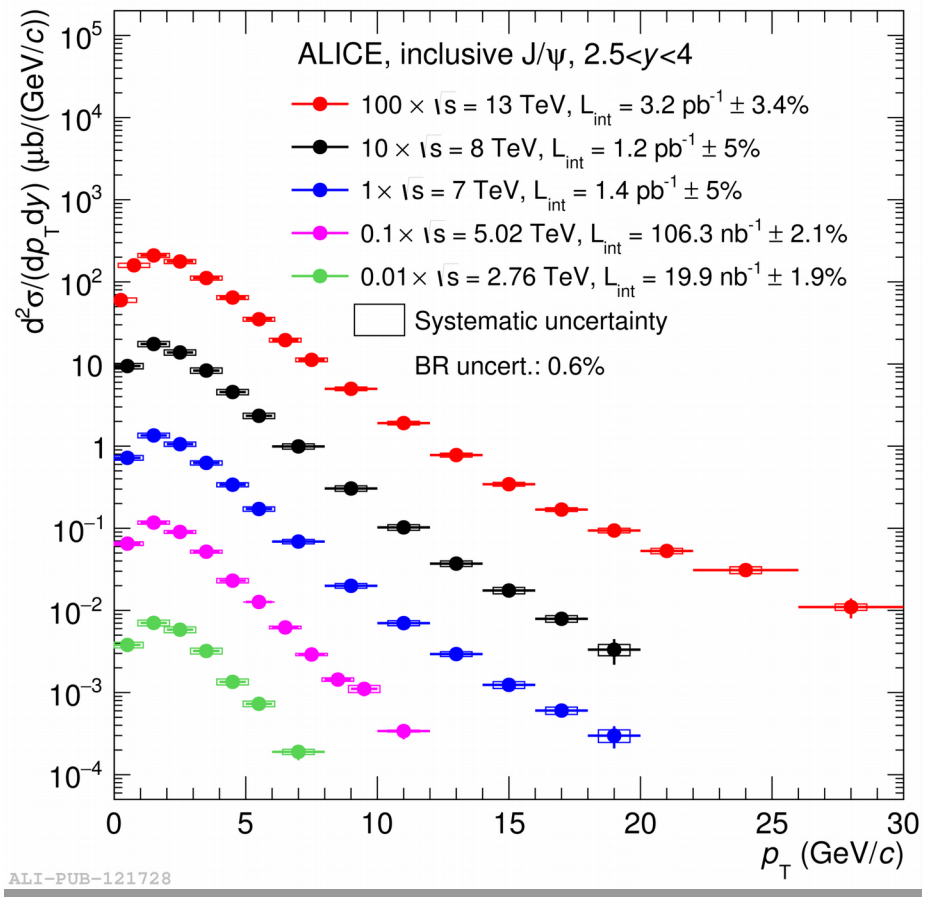

√s = 2.76 TeV	PLB 718 (2012) 295
Run2 New √s = 5 TeV	PLB 766 (2017) 212
√s = 7 TeV	EPJC 74 (2014) 2974
√s = 8 TeV	EPJC 76 (2016) 18
Run2 New √s = 13 TeV	EPJC 77 (2017) 392

Comparison to ALICE inclusive measurements at √s = 2.76, 5, 7 and 8 TeV

Steady increase of the luminosity and p_T reach with increasing energy

As expected, spectra becomes harder with increasing energy

Change of slope at high p_T and √s = 13 TeV, attributed to the onset of the non-prompt J/ψ contribution

Both the broadening and the change of slope can also be characterized by mean p_T measurements

Comparison to lower energy: J/ψ vs p_T

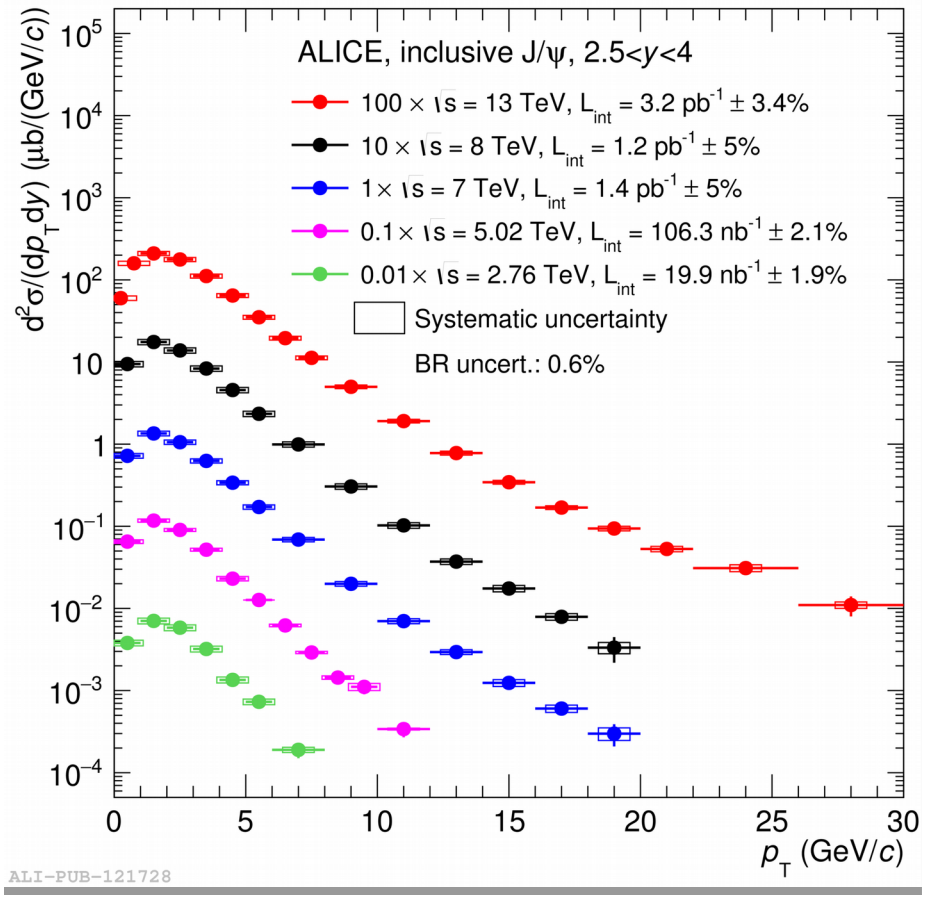

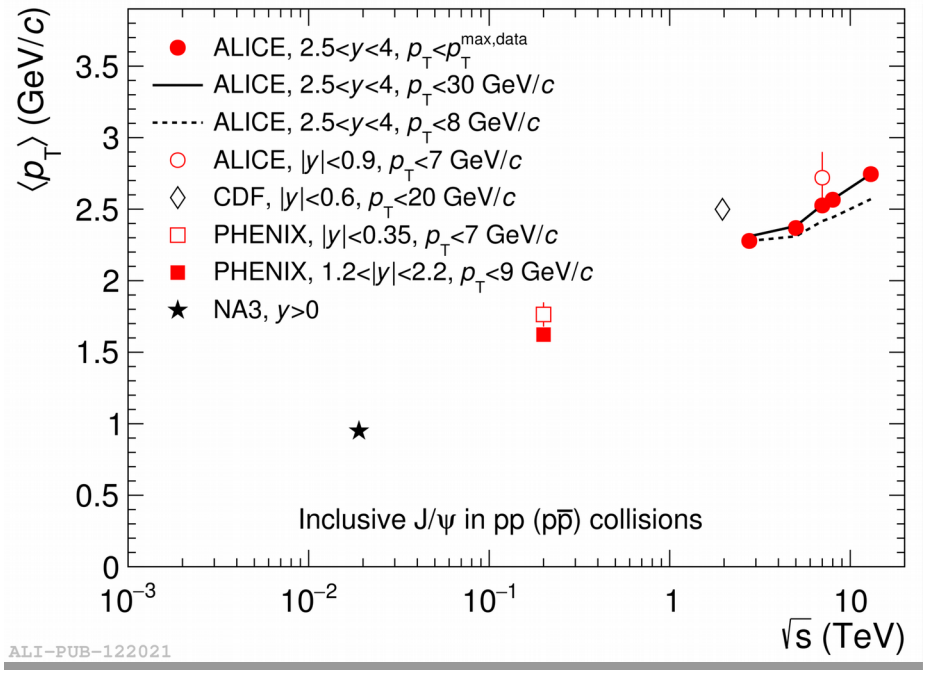

<p_T> is measured using fits to the p_T distributions.

A steady increase of <p_T> with increasing √s .

Values at mid- are systematically larger than at forward-rapidity.

Could be attributed to an increase in the longitudinal momentum at forward-rapidity leaving less energy available in the transverse plane.

√s = 2.76 TeV	PLB 718 (2012) 295
Run2 New √s = 5 TeV	PLB 766 (2017) 212
√s = 7 TeV	EPJC 74 (2014) 2974
√s = 8 TeV	EPJC 76 (2016) 18
Run2 New √s = 13 TeV	EPJC 77 (2017) 392

Models

$$d\sigma^{Q} = f_a(x_a)\, f_b(x_b) \times d\hat{\sigma}_{ab}^{q\bar{q}} \times \left\langle O_{q\bar{q}}^{Q} \right\rangle$$

Three main approaches are used to describe direct charmonium production in pp

- Color Evaporation Model (CEM):
  production cross section of a given charmonium is proportional to the $c\bar{c}$ cross section, integrated between the mass of the charmonium and twice the mass of the lightest D meson. Proportionality factor is independent of y, p_T and $\sqrt{s}$
- Color Singlet model (CSM):
  pQCD is used to describe the $c\bar{c}$ production with the same quantum numbers (CS) as the final-state meson. The hadronization term becomes simpler and is calculated using lattice QCD
- Non-Relativistic QCD (NRQCD):
  Both CS and CO state of the $c\bar{c}$ pairs are considered. The relative contribution of the states is parametrized using a finite set of universal long distance matrix elements (LDME), fitted to a subset of the data (e.g. Tevatron)

Models

$$d\sigma^{Q} = f_a(x_a)\, f_b(x_b) \times d\hat{\sigma}_{ab}^{q\bar{q}} \times \left\langle O_{q\bar{q}}^{Q} \right\rangle$$

Three main approaches are used to describe direct charmonium production in pp

- Color Evaporation Model (CEM):
  production cross section of a given charmonium is proportional to the $c\bar{c}$ cross section, integrated between the mass of the charmonium and twice the mass of the lightest D meson. Proportionality factor is independent of y, p_T and $\sqrt{s}$
- Color Singlet model (CSM):
  pQCD is used to describe the $c\bar{c}$ production with the same quantum numbers (CS) as the final-state meson. The hadronization term becomes simpler and is calculated using lattice QCD
- Non-Relativistic QCD (NRQCD):
  Both CS and CO state of the $c\bar{c}$ pairs are considered. The relative contribution of the states is parametrized using a finite set of universal long distance matrix elements (LDME), fitted to a subset of the data (e.g. Tevatron)

Models

$$d\sigma^{Q} = f_a(x_a)\, f_b(x_b) \times d\hat{\sigma}_{ab}^{q\bar{q}} \times \left\langle O_{q\bar{q}}^{Q} \right\rangle$$

Three main approaches are used to describe direct charmonium production in pp

- Color Evaporation Model (CEM):
  production cross section of a given charmonium is proportional to the $c\bar{c}$ cross section, integrated between the mass of the charmonium and twice the mass of the lightest D meson. Proportionality factor is independent of y, p_T and $\sqrt{s}$
- Color Singlet model (CSM):
  pQCD is used to describe the $c\bar{c}$ production with the same quantum numbers (CS) as the final-state meson. The hadronization term becomes simpler and is calculated using lattice QCD
- Non-Relativistic QCD (NRQCD):
  Both CS and CO state of the $c\bar{c}$ pairs are considered. The relative contribution of the states is parametrized using a finite set of universal long distance matrix elements (LDME), fitted to a subset of the data (e.g. Tevatron)

Non-prompt contribution corresponds to the production of b-hadrons. Can be calculated with pQCD, e.g. within FONLL

Inclusive results compared to NRQCD

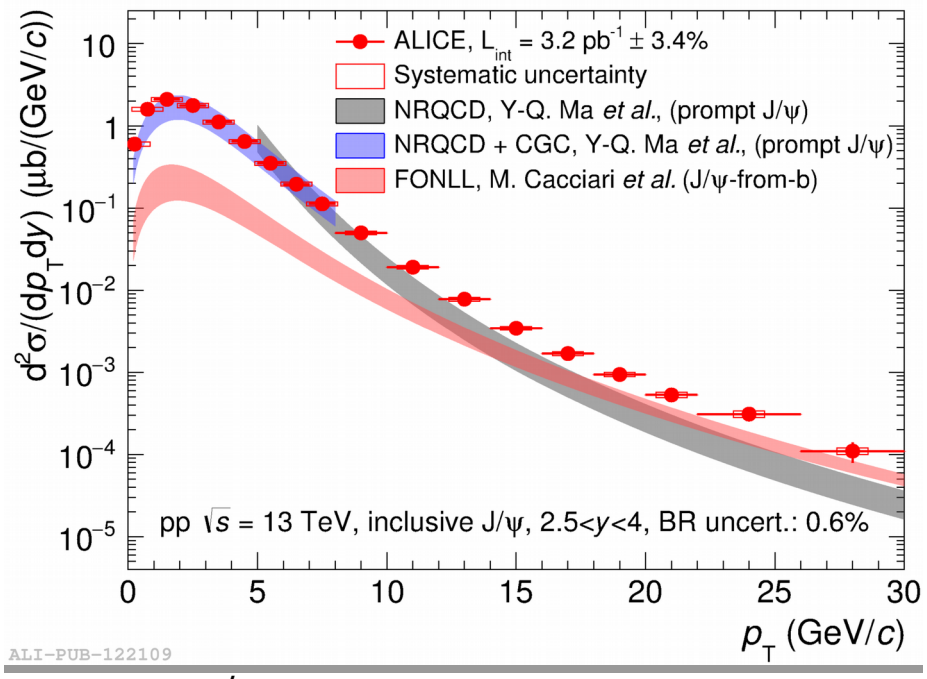

J/ψ vs p_T at √s=13 TeV

NRQCD	Ma, Wang and Chao, PRL 106 (2011) 042002
NRQCD+CGC	Ma and Venugopalan, PRL 113 (2014) 192301
FONLL	Cacciari *et al.*, JHEP 1210 (2012) 137

Models properly account for higher mass resonance decays

At low p_T, NRQCD is coupled to a CGC description of the proton:

In this region the contribution from non prompt is small (<10%) and the CGC+NRQCD calculation reproduces the data well.

At high p_T, non-prompt J/ψ constitute a sizable contribution to the inclusive cross section

Eur. Phys. J. C 77 (2017) 392

Inclusive results compared to NRQCD

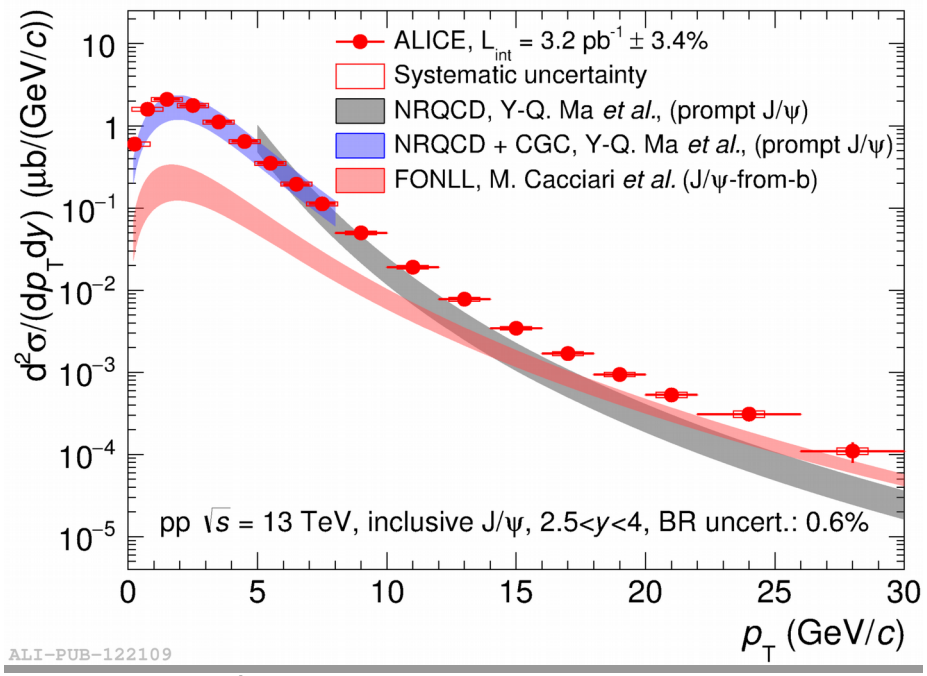

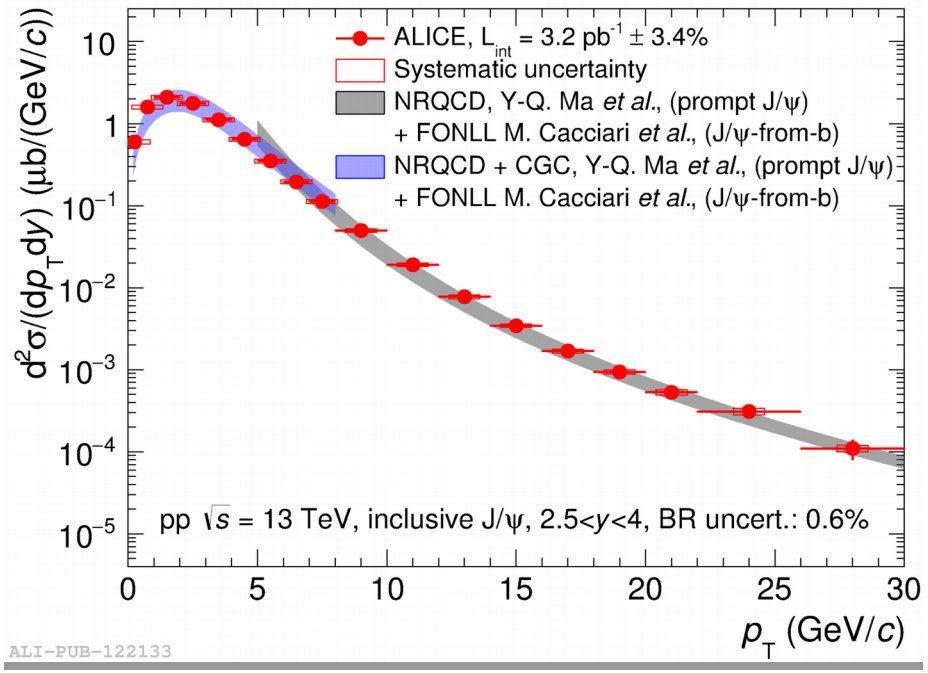

J/ψ vs p_T @ √s=13 TeV

NRQCD	Ma, Wang and Chao, PRL 106 (2011) 042002
NRQCD+CGC	Ma and Venugopalan, PRL 113 (2014) 192301
FONLL	Cacciari *et al.*, JHEP 1210 (2012) 137

Right Fig.: Summed NRQCD and FONLL calculations assuming fully uncorrelated uncertainties.

Agreement with the data over the full p_T range and 5 orders of magnitude in σ

Eur. Phys. J. C 77 (2017) 392

Data at all energies vs p_T compared to NRQCD

Extensive data-theory comparisons done at all energies available at the LHC so far.

Good agreement between the model and the data is observed for all measured cross sections, for both J/ψ and ψ(2S)

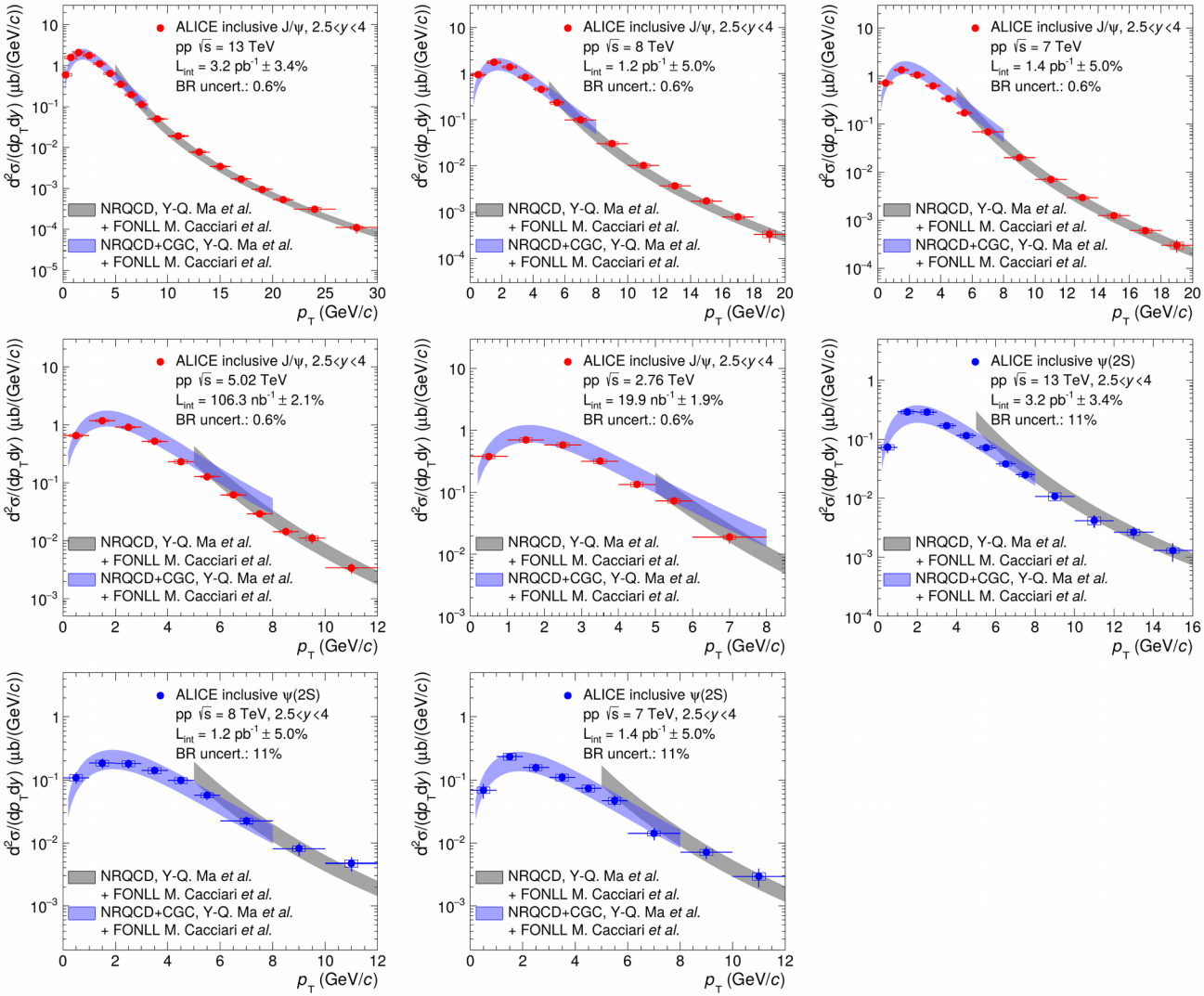

Eur. Phys. J. C 77 (2017) 392

Data at all energies vs y compared to NRQCD

Extensive data-theory comparisons done at all energies available at the LHC so far.

Good agreement between the model and the data is observed for all measured cross sections, for both J/ψ and ψ(2S)

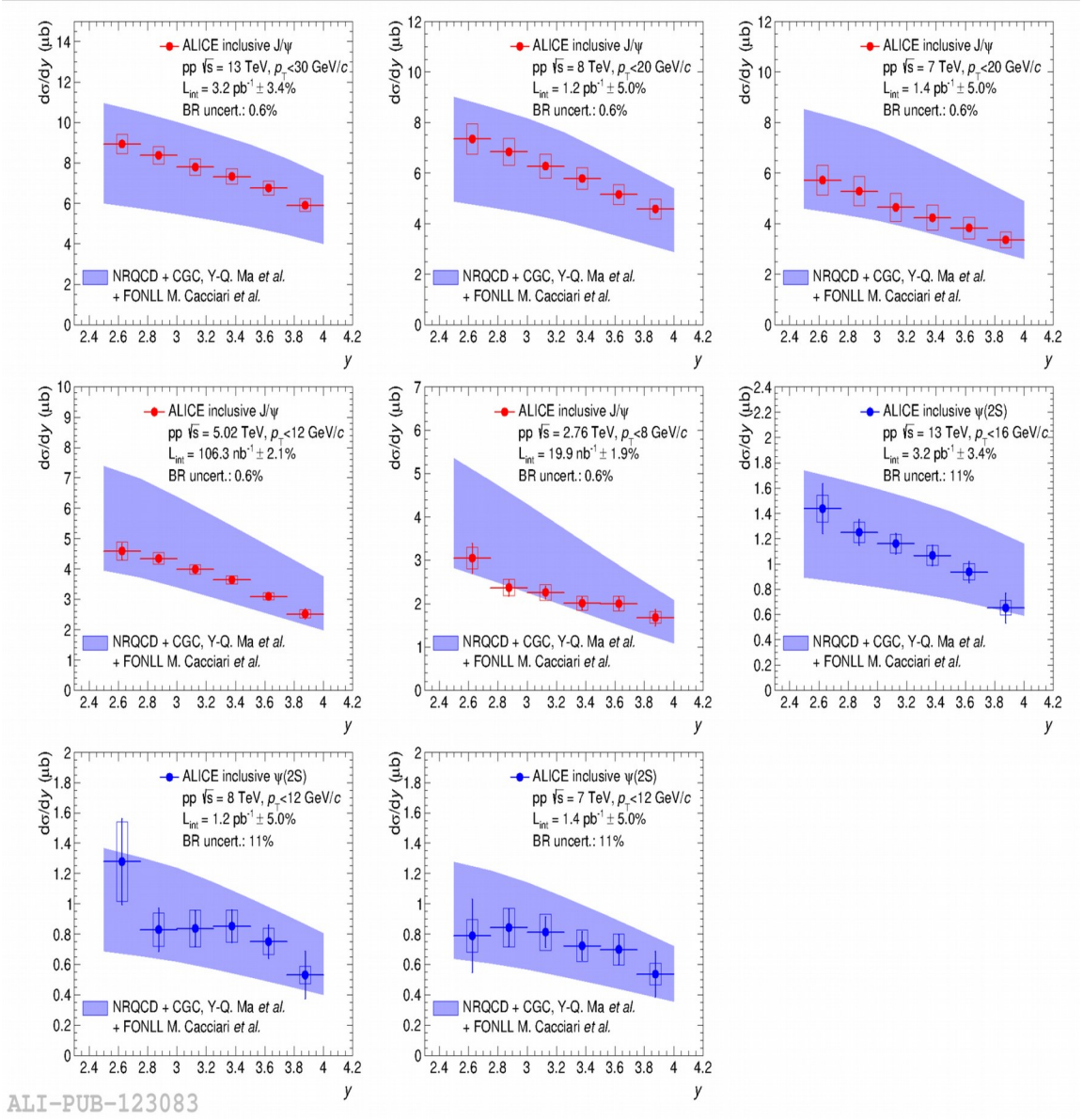

Eur. Phys. J. C 77 (2017) 392

J/ψ production in **p-Pb** collisions at $\sqrt{s_{NN}}$ = 8.16 TeV

J/ψ production in p-Pb at $\sqrt{s_{NN}}$ = 8.16 TeV

Two colliding beam configurations: p-Pb and Pb-p, $2.5<y_{LAB}<4$

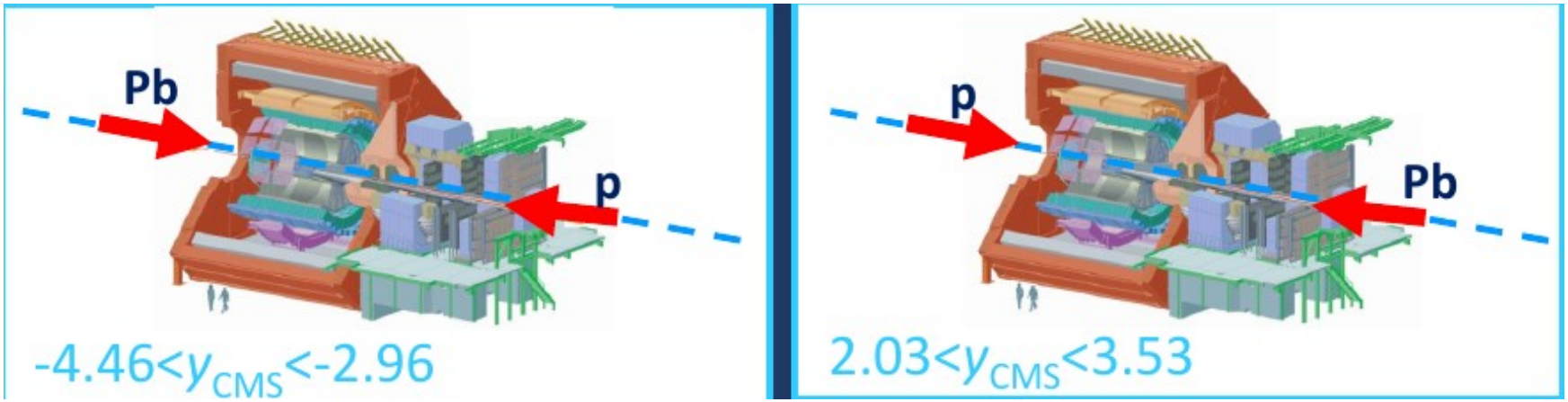

$1.1 \times 10^{-5} < x < 5 \times 10^{-5}$ (p-going)
$7.3 \times 10^{-3} < x < 3.3 \times 10^{-2}$ (Pb-going)

p-Pb L_{int} ~8.7 nb^{-1}
Pb-p L_{int} ~12.9 nb^{-1}

J/ψ production in p-Pb at $\sqrt{s_{NN}}$ = 8.16 TeV

R_{pPb} vs y

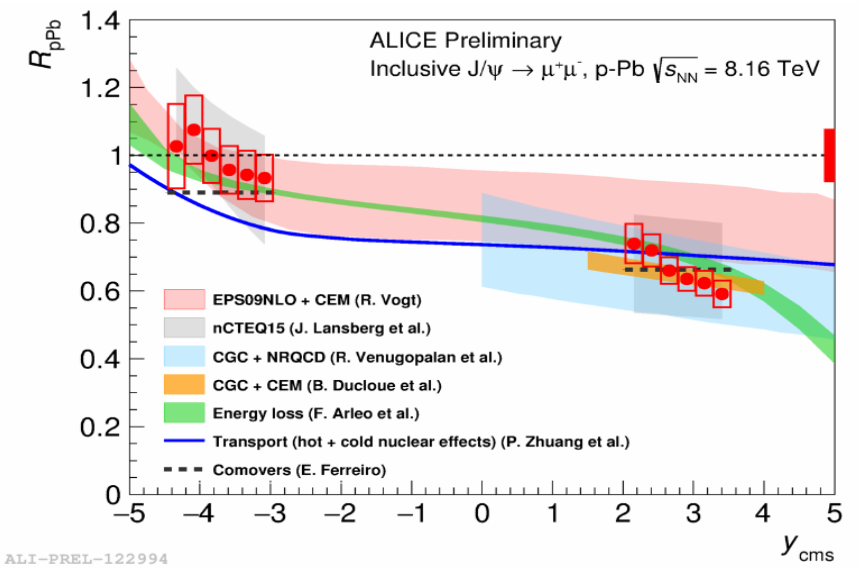

p_T extended from 7 to 20 GeV/*c* from previous RUN1 result (JHEP 02 (2014) 073)

Agreement between data and models within the current experimental and theoretical uncertainties.

- pdf modifications
- Color glass condensate
- Energy loss
- Final state effects:
  - Transport: thermal rate eq. with continuous J/ψ dissociation and regeneration
  - Comovers: J/ψ dissociated via interactions with partons

.

$1.1 \times 10^{-5} < x < 5 \times 10^{-5}$ (p-going)
$7.3 \times 10^{-3} < x < 3.3 \times 10^{-2}$ (Pb-going)

J/ψ production in p-Pb at $\sqrt{s_{NN}}$ = 8.16 TeV

R_{pPb} vs p_T

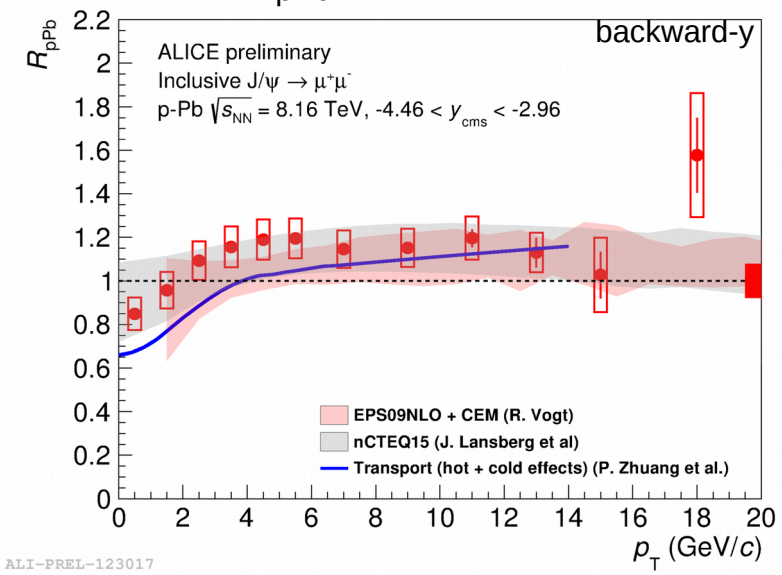

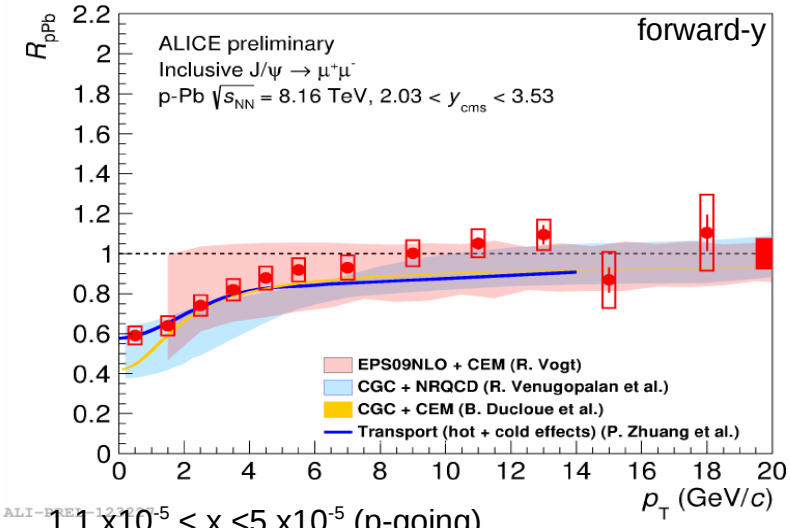

$1.1 \times 10^{-5} < x < 5 \times 10^{-5}$ (p-going)
$7.3 \times 10^{-3} < x < 3.3 \times 10^{-2}$ (Pb-going)

p_T extended from 7 to 20 GeV/c from previous RUN1 result (JHEP 02 (2014) 073)

Agreement between data and models within the current experimental and theoretical uncertainties.

- pdf modifications
- Color glass condensate
- Energy loss
- Final state effects:
  - Transport: thermal rate eq. with continuous J/ψ dissociation and regeneration
  - Comovers: J/ψ dissociated via interactions with partons

.

New: J/ψ Q_{pPb} as a function of centrality class at $\sqrt{s_{NN}}$=8.16 TeV

Forward rapidity:
Larger suppression observed with larger N_{coll}

Backward rapidity:
Less suppression observed with larger N_{coll}

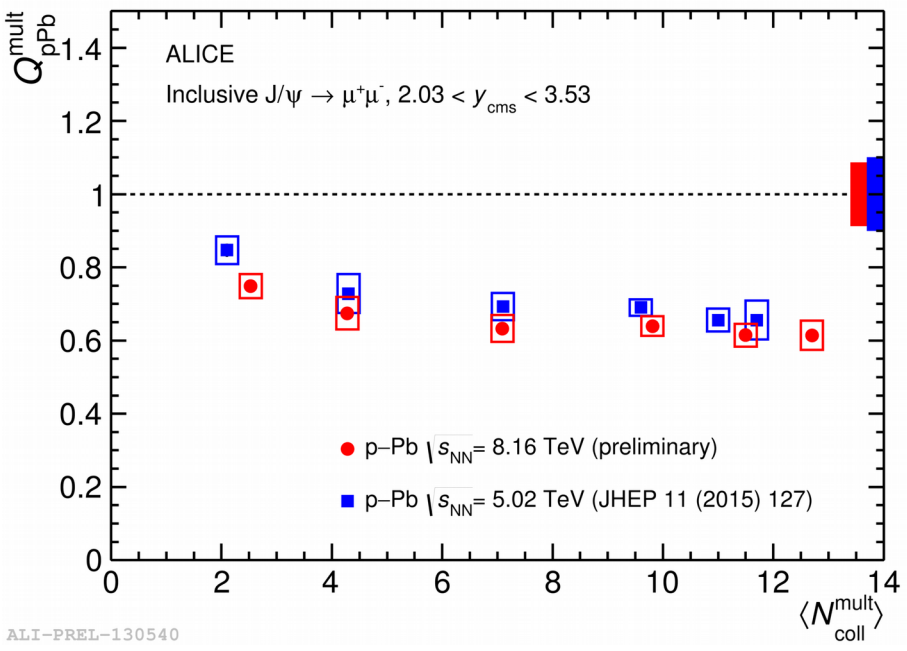

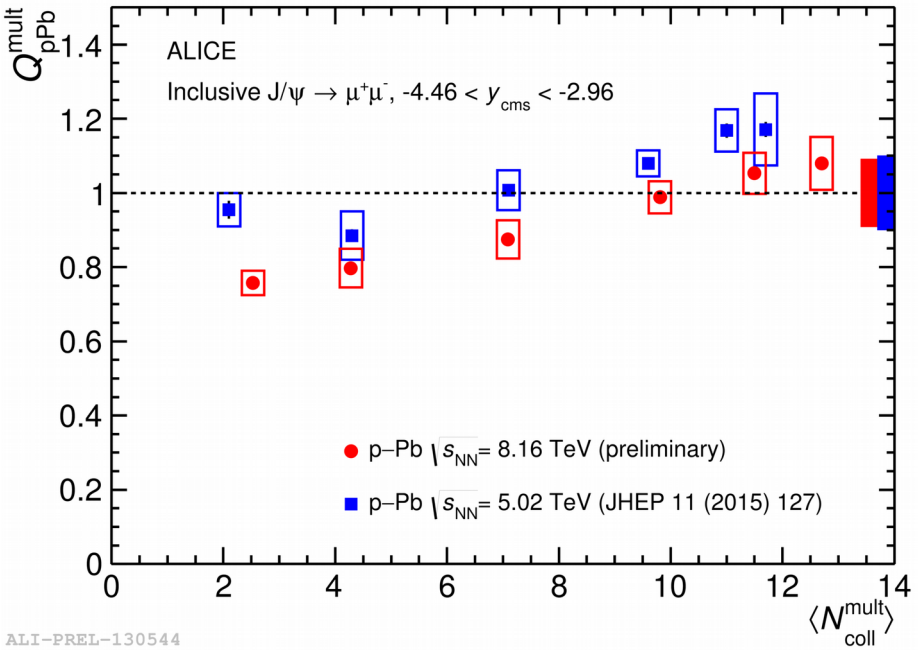

Results compatible with those measured by ALICE at $\sqrt{s_{NN}}$ = 5.02 TeV
JHEP 11 (2015) 127

CERN-ALICE-PUBLIC-2017-007
PRC91 (2015) 064905 (Centrality determination)

Summary

Inclusive J/ψ and ψ(2S) production in pp collisions at several √*s*

J/ψ: the results are consistent between ALICE and LHCb.

ψ(2S): ALICE is the only measurement available at $\sqrt{s}$ =13 TeV down to p_T =0

Data can be well reproduced

- at low p_T by a model that couples a CGC description of the proton to NRQCD
- at intermediate and high-p_T by NRQCD calculations (and FONLL for the non-prompt contributions)

Inclusive J/ψ production in p-Pb collisions at $\sqrt{s_{NN}}$ = 8.16 TeV

Larger suppression observed in more central collisions at forward rapidity, opposite trend observed at backward rapidity

Centrality integrated results are compatible with several models that include cold nuclear matter effects as well as final state interactions, within uncertainties

Results are compatible with those measured by ALICE at $\sqrt{s_{NN}}$=5.02 TeV.

Extras

Data analysis

Quarkonia are measured using fits to the invariant mass distribution of $\mu^+\mu^-$ pairs detected in the muon system at forward rapidity or the e^+e^- pairs at central rapidity

pp@13 TeV data sample from 2015 run at LHC

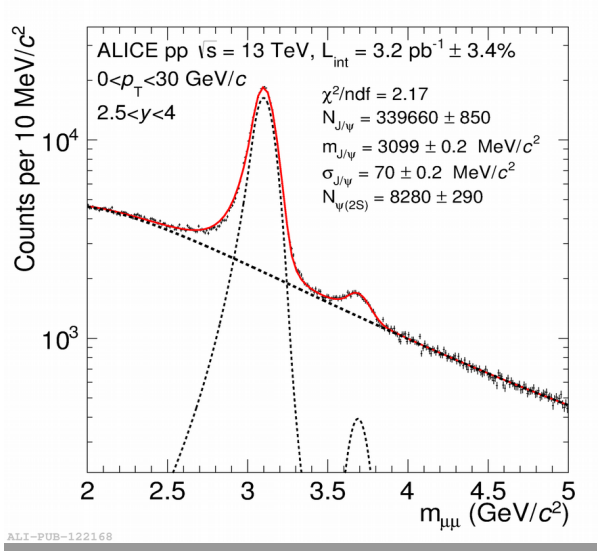

Forward rapidity

Central rapidity

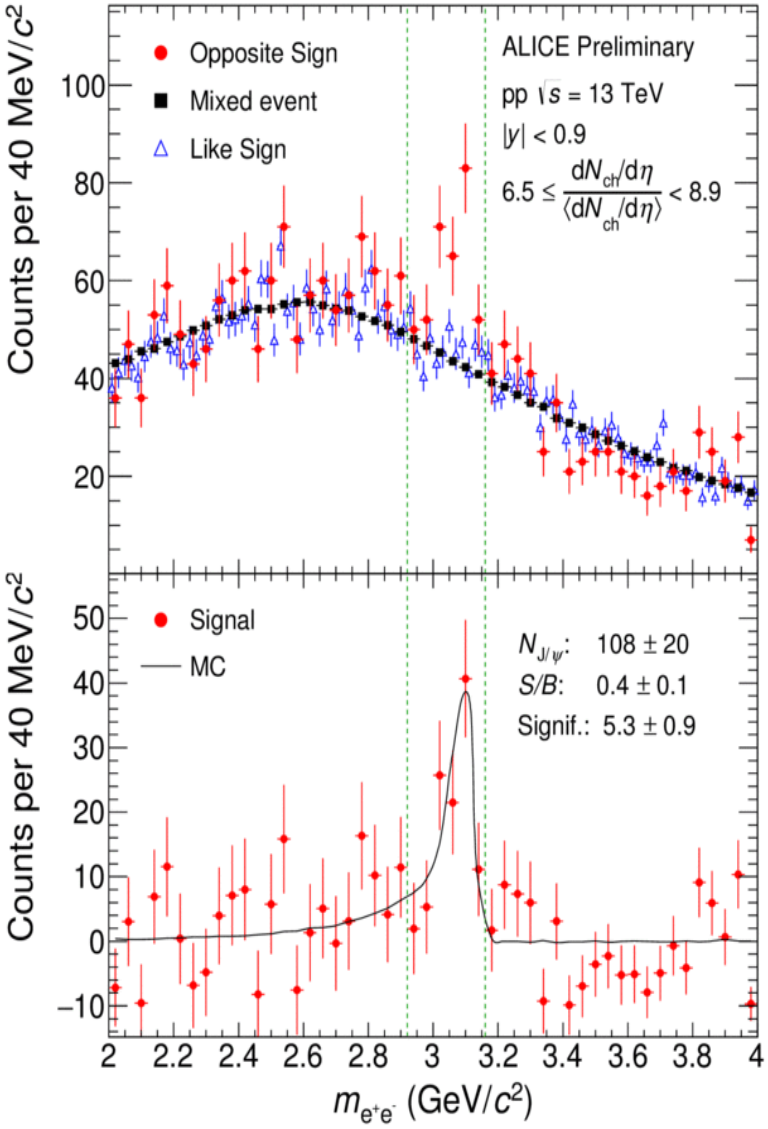

Outlook

Inclusive J/ψ at $\sqrt{s}$ =13TeV shows a large contribution from non-prompt J/ψ to the inclusive cross sections observed for high p_T

Today it is impossible at ALICE to separate prompt J/ψ from the non-prompt coming from B-mesons decays.

The Muon Forward Tracker (MFT) will allow (among other things) to separate prompt and non prompt J/ψ, but also to improve the precision of J/ψ and ψ(2S) measurements, to measure separately D and B mesons, etc.

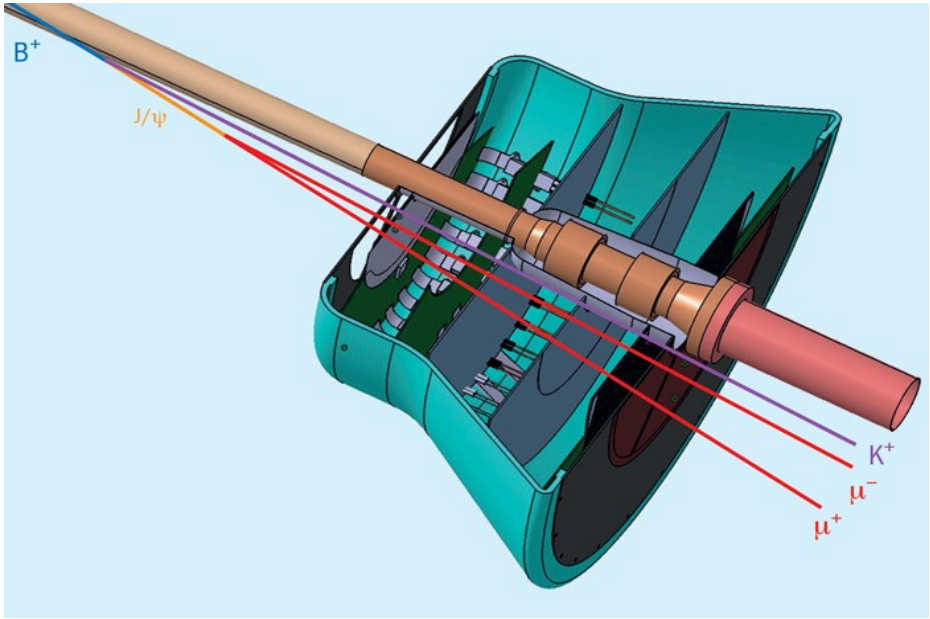

Comparison to lower energy: ψ(2S) vs p_T

inclusive J/ψ

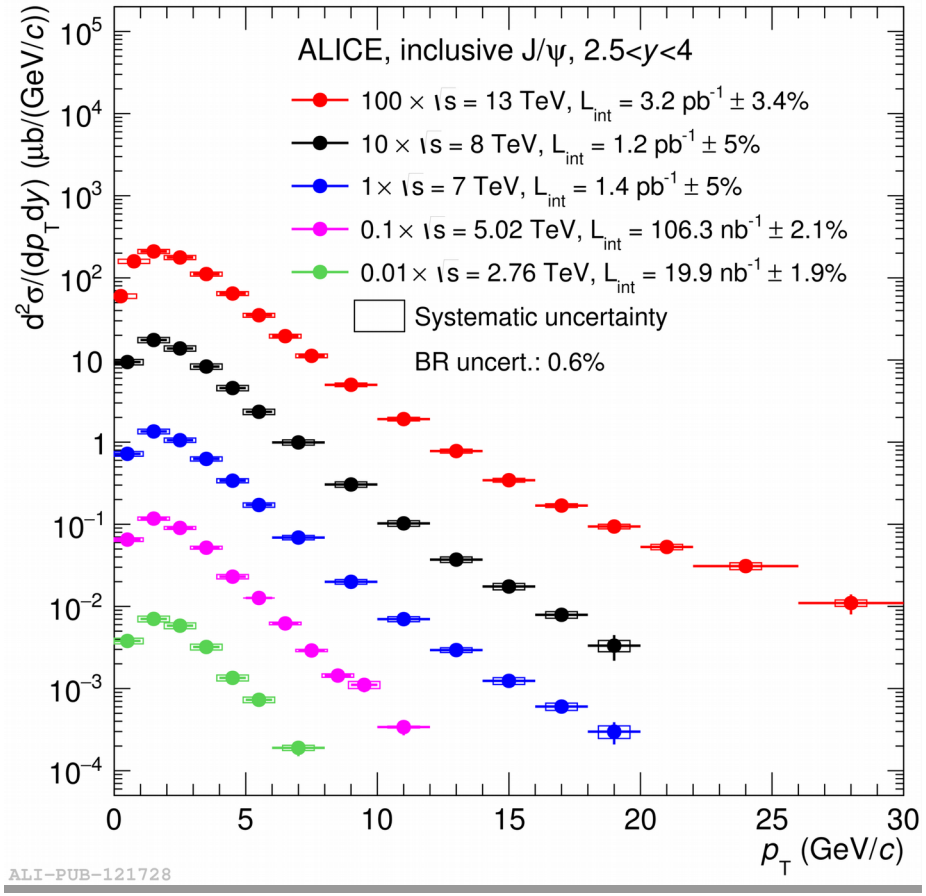

inclusive ψ(2S)

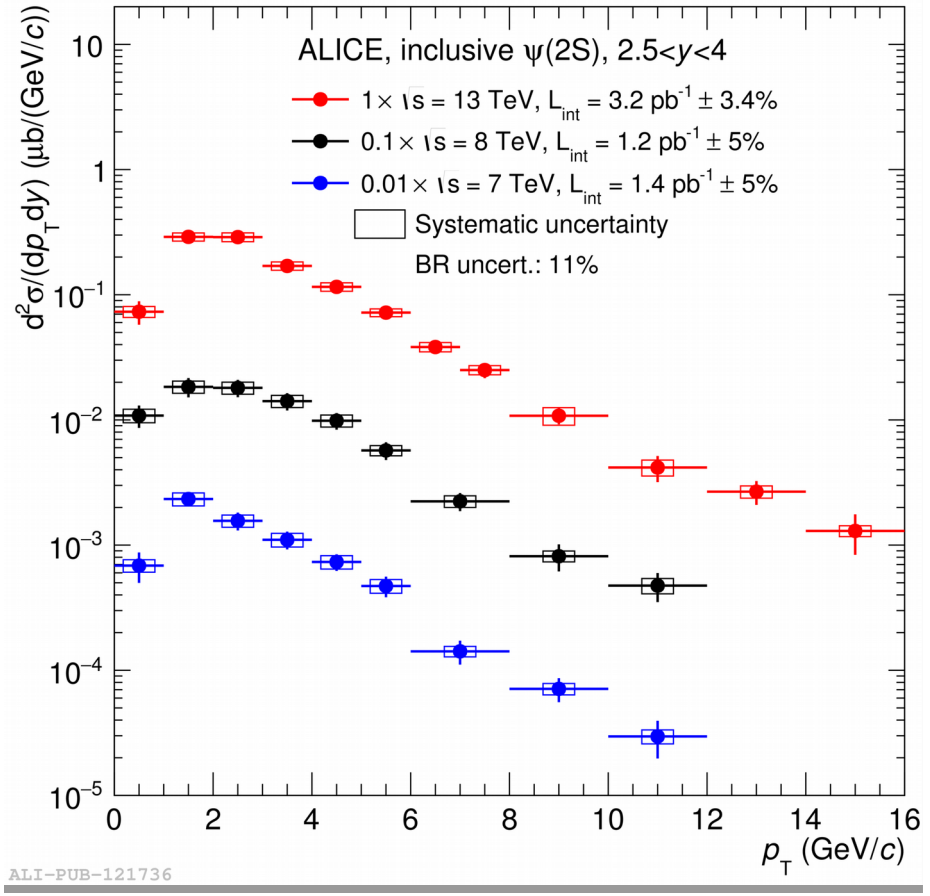

√s = 2.76 TeV PLB 718 (2012) 295
√s = 5 TeV PLB 766 (2017) 212
√s = 7 TeV EPJC 74 (2014) 2974
√s = 8 TeV EPJC 76 (2016) 18
√s = 13 TeV ArXiv:1702.00557

For ψ(2S) ALICE measurements available at √s = 7, 8 and 13 TeV

Comparison to lower energy: J/ψ and ψ(2S) vs *y*

inclusive J/ψ

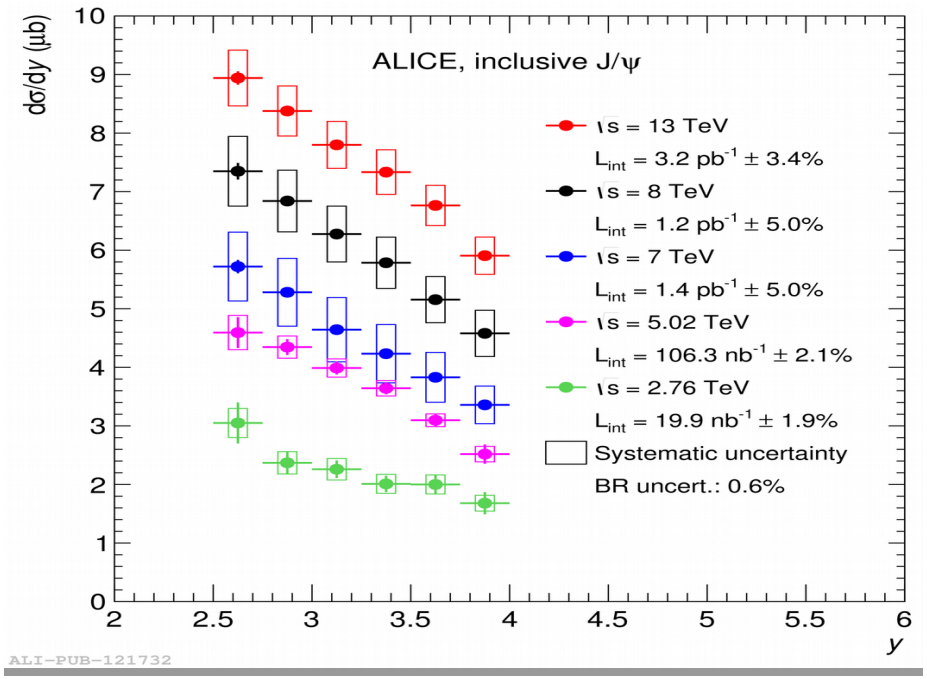

inclusive ψ(2S)

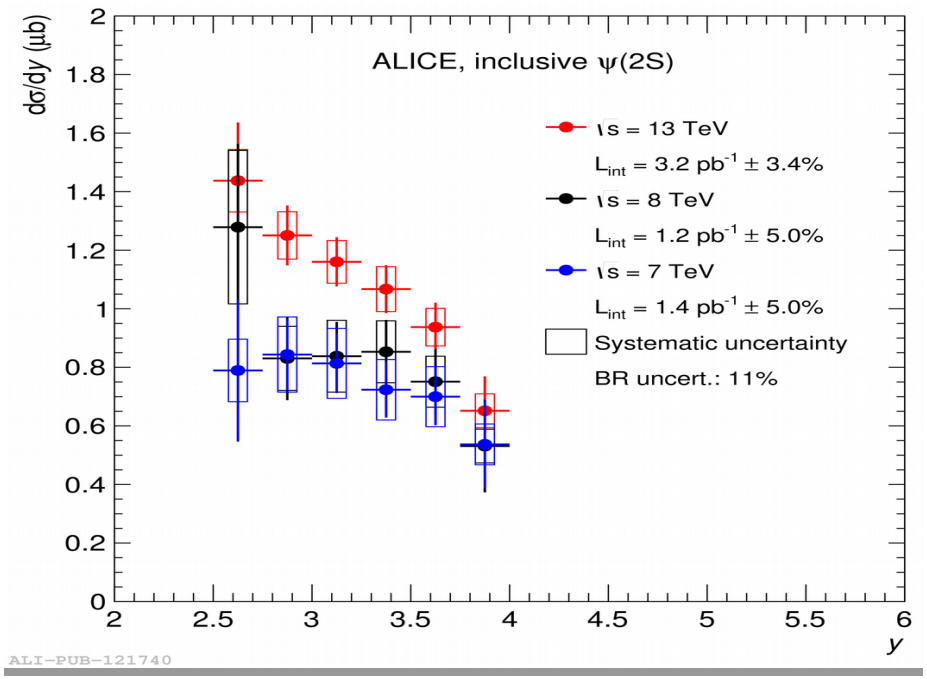

√*s* = 2.76 TeV	PLB 718 (2012) 295
√*s* = 5 TeV	ArXiv:1606.08197
√*s* = 7 TeV	EPJC 74 (2014) 2974
√*s* = 8 TeV	EPJC 76 (2016) 18
√*s* = 13 TeV	ArXiv:1702.00557

For J/ψ, no visible change in the *y* distribution

For ψ(2S), large uncertainties prevent firm conclusions

Particle ratios, energy dependence

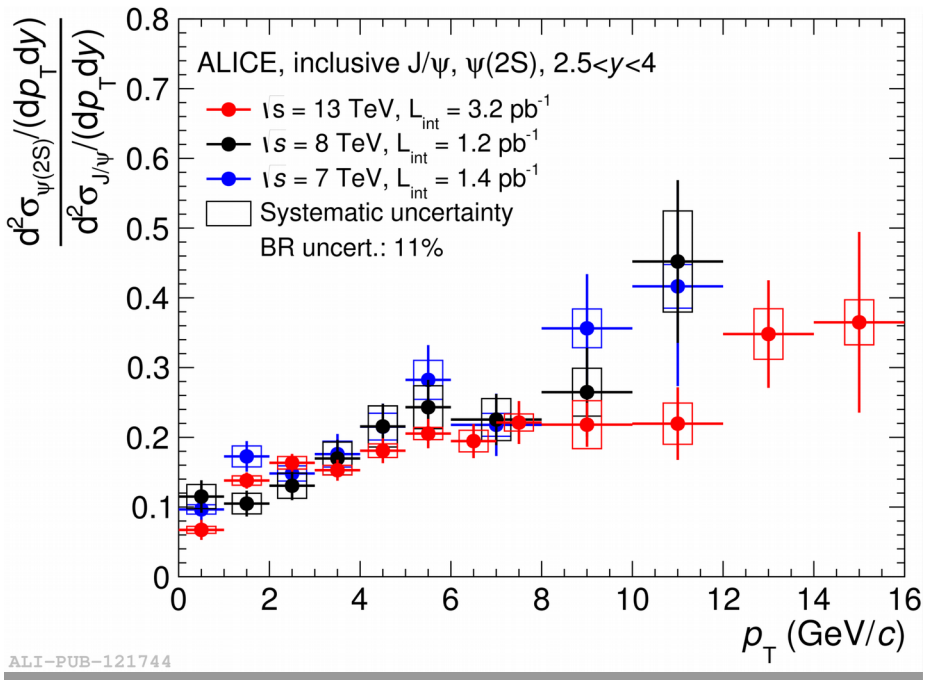

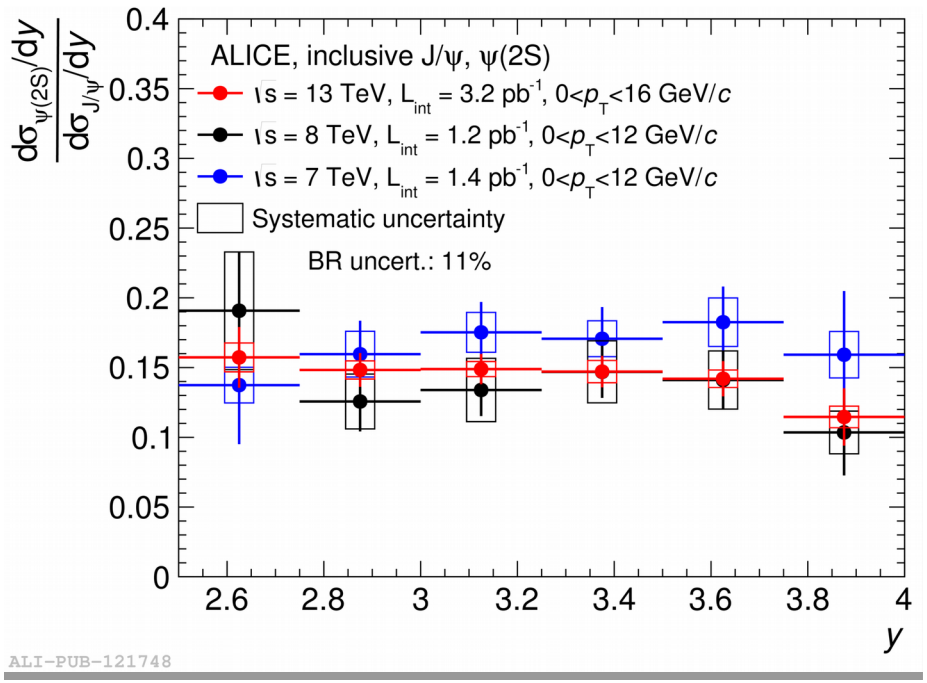

No visible √*s* dependence of the p_T-differential ψ(2S)-to-J/ψ ratio

No clear trend either vs rapidity

Mean p_T energy dependence

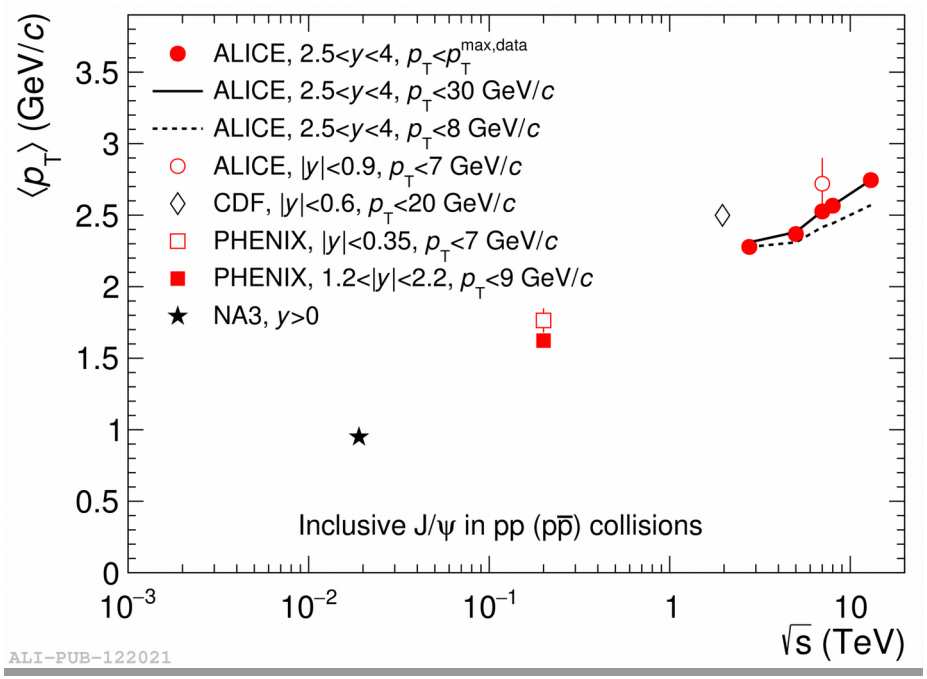

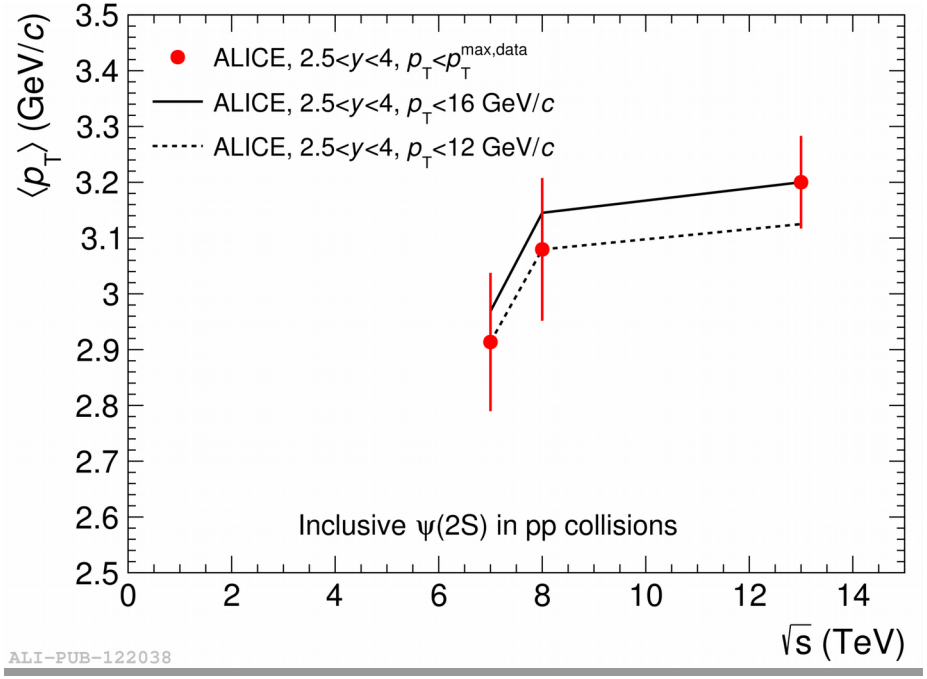

<p_T> is measured using fits to the p_T distributions.

A steady increase of <p_T> with increasing $\sqrt{s}$.

Consistent with the expected hardening of the of the J/ψ and ψ(2S) p_T distributions.

Values at mid- are systematically larger than at forward-rapidity.

Could be attributed to an increase in the longitudinal momentum at forward-rapidity leaving less energy available in the transverse plane.

Inclusive results compared to NRQCD

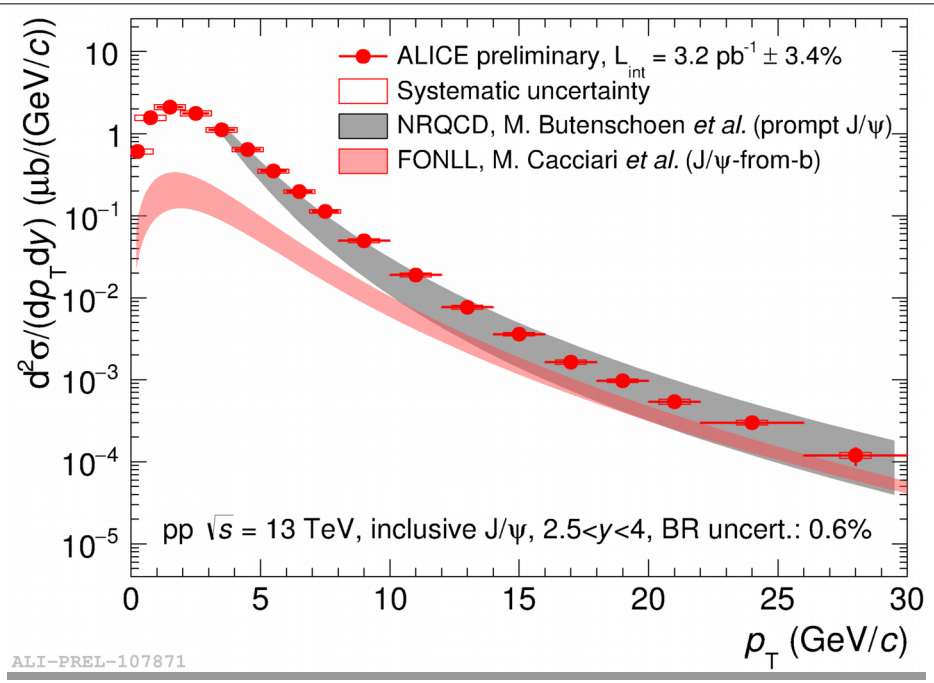

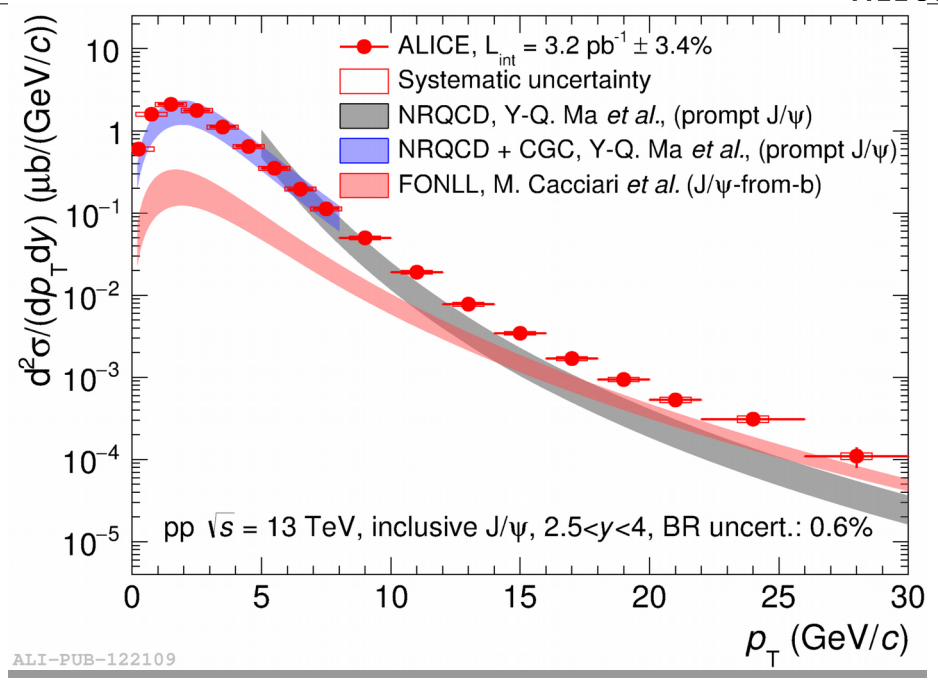

J/ψ vs p_T @13 TeV

NRQCD (left)	Butenschoen and Kniehl, PRL 106 (2011) 022003
NRQCD (right)	Ma, Wang and Chao, PRL 106 (2011) 042002
NRQCD+CGC	Ma and Venugopalan, PRL 113 (2014) 192301
FONLL	Cacciari *et al.*, JHEP 1210 (2012) 137

All models properly account for higher mass resonance decays

NRQCD models differ in the set of LRME that is used, the p_T at which fits are performed and the datasets considered.

At low p_T (right), NRQCD is coupled to a CGC description of the proton

Predictions are quite different at high p_T, but in both cases, non-prompt J/ψ constitute a sizable contribution to the inclusive cross section

Inclusive results compared to NRQCD

Summed NRQCD and FONLL calculations assuming fully uncorrelated uncertainties.

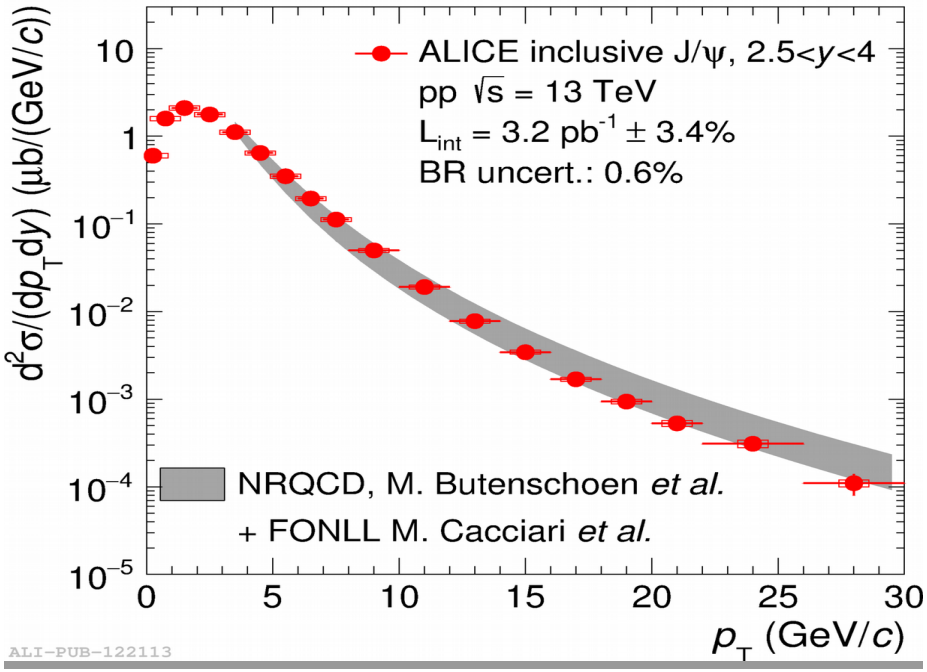

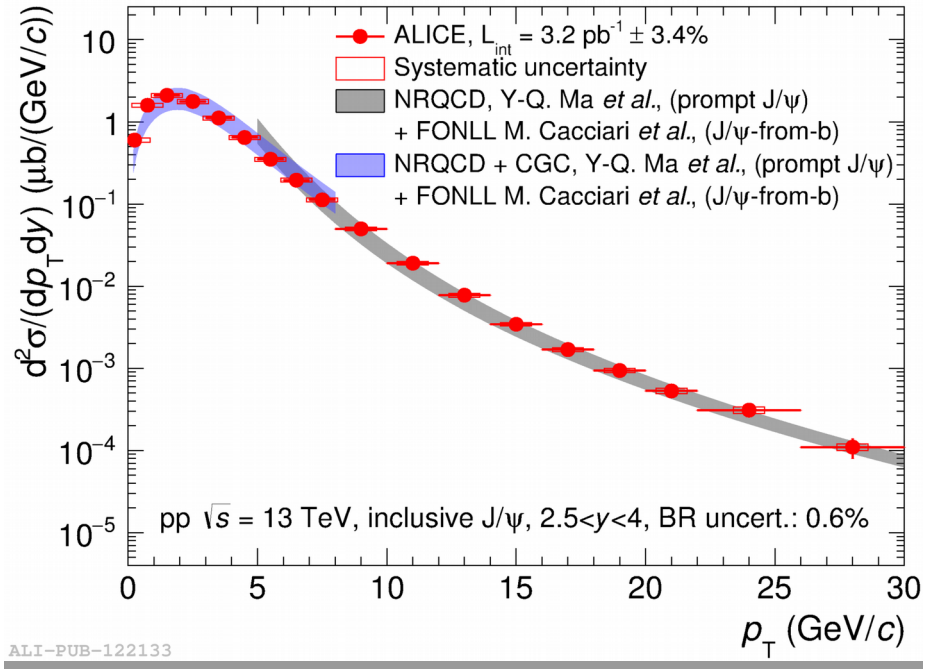

Agreement to the data is much improved, already at intermediate p_T and especially for the calculation from Ma *et al.*

Note that the calculations are completely independent, and that there was no data at this energy, this rapidity and at such high p_T before

Comparison to NRQCD: ψ(2S) vs p_T

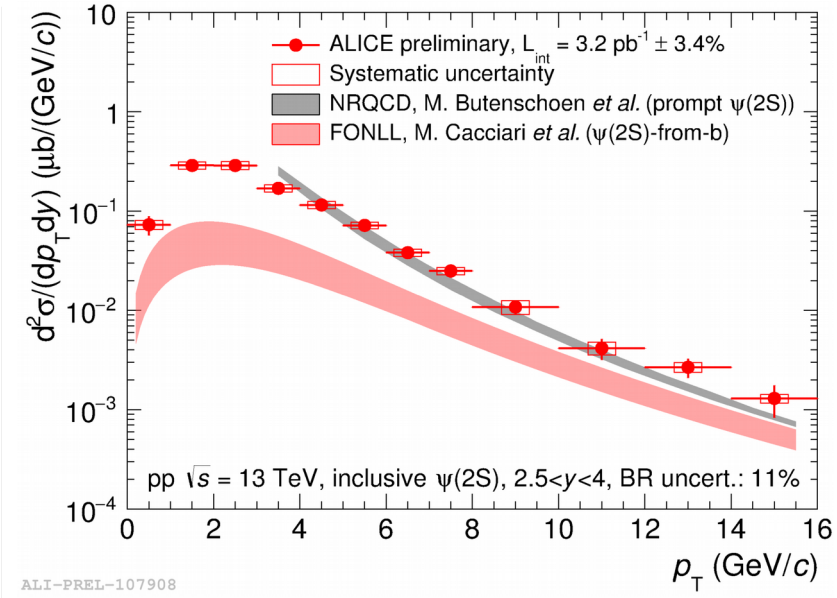

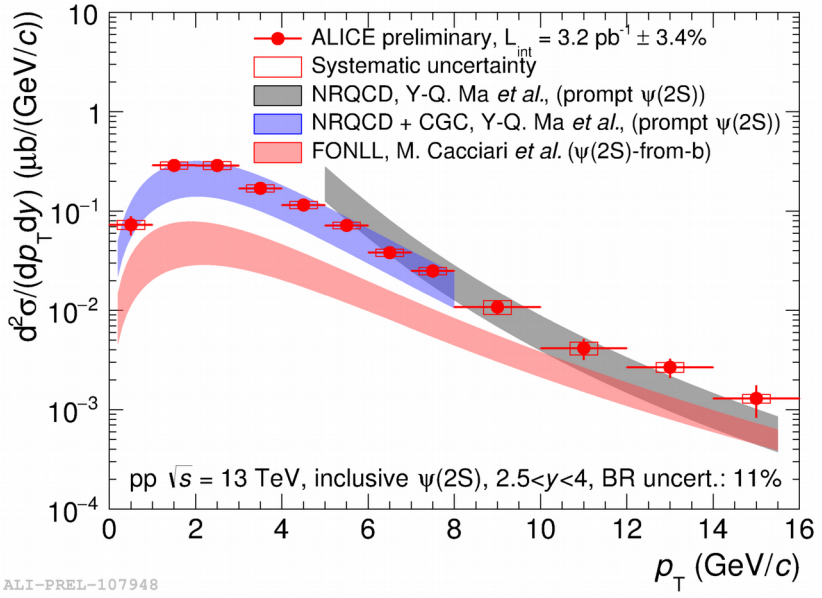

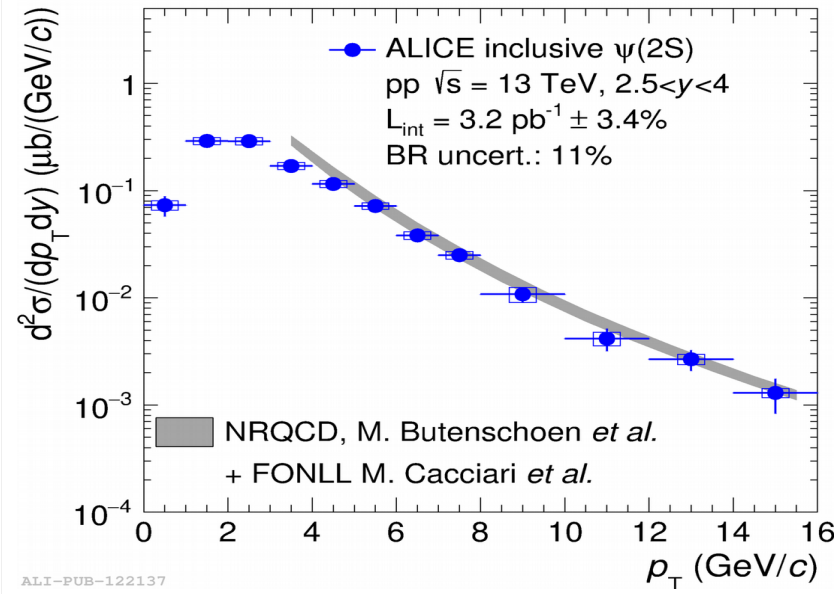

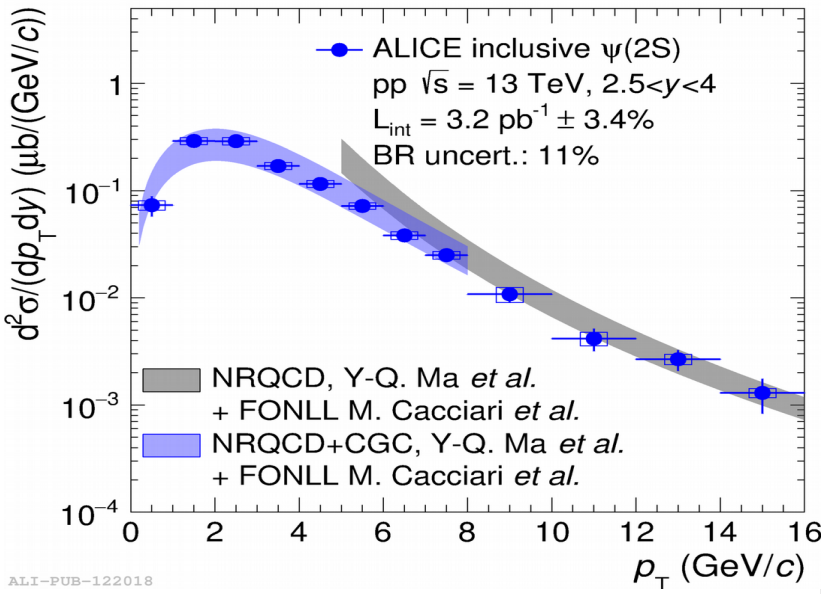

Same conclusions as for the J/ψ case

Rapidity distributions

Since the NRQCD+CGC calculation goes down to *p*T = 0, it can be compared to our *p*T-integrated data vs rapidity

Ma and Venugopalan, PRL 113 (2014) 192301

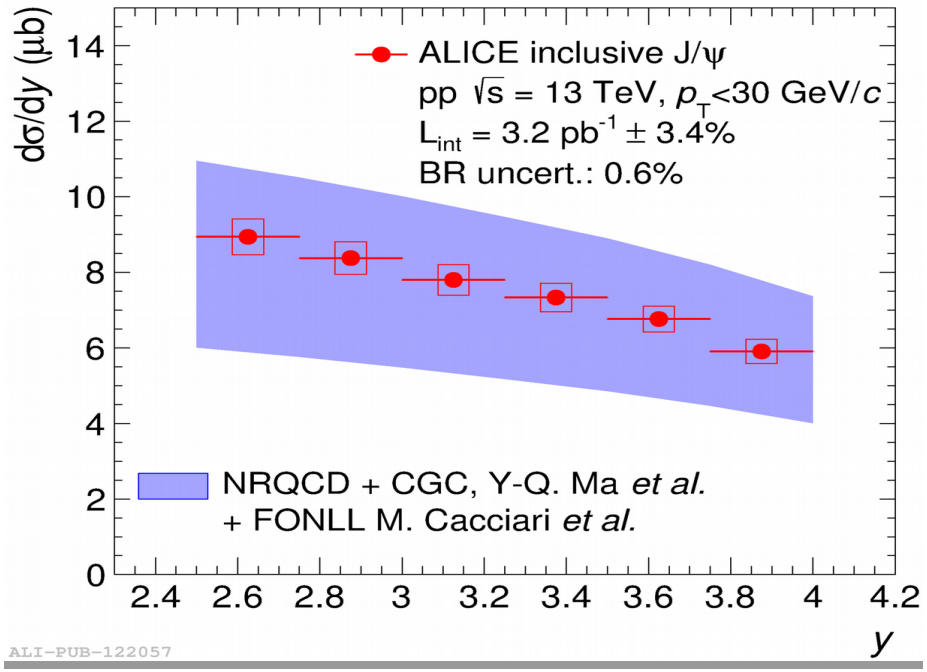

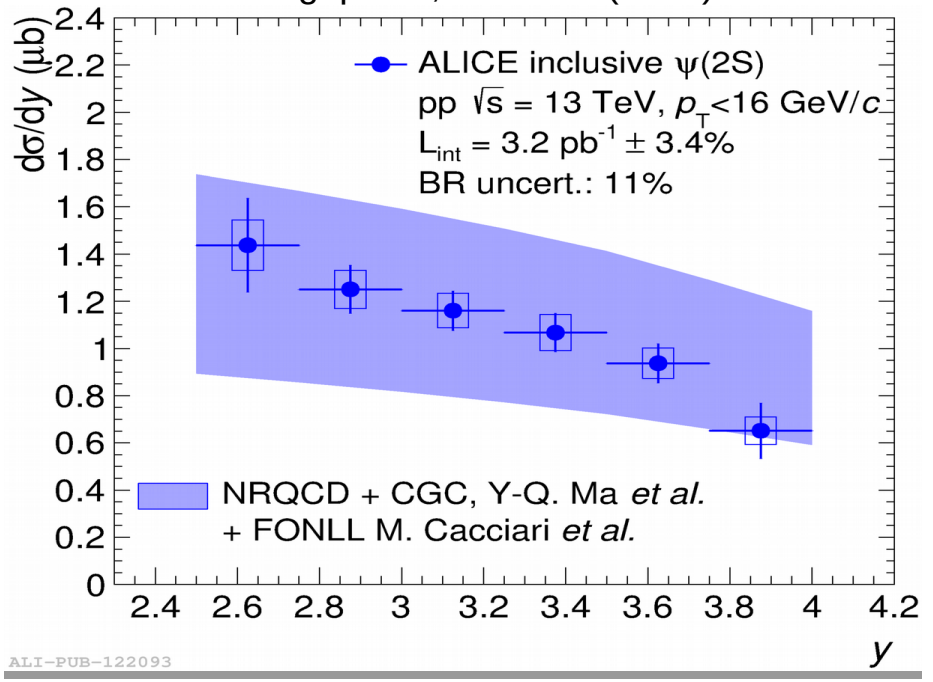

Agreement to the data is reasonable

The only other calculation that provides p_T-integrated rapidity distributions is CSM@LO, with significantly larger uncertainties (see ALICE (7TeV) EPJC 74 (2014) 2974 and backups)

dσ/dy as a function of √*s*

Steady increase of dσ/dy as a function of increasing √*s*.

The J/ψ cross sections are compared to a calculation done in the CEM framework (PRC 87 014908)

Data lie on the upper side of the calculation and the difference to the central value becomes larger with increasing √*s*.

inclusive J/ψ

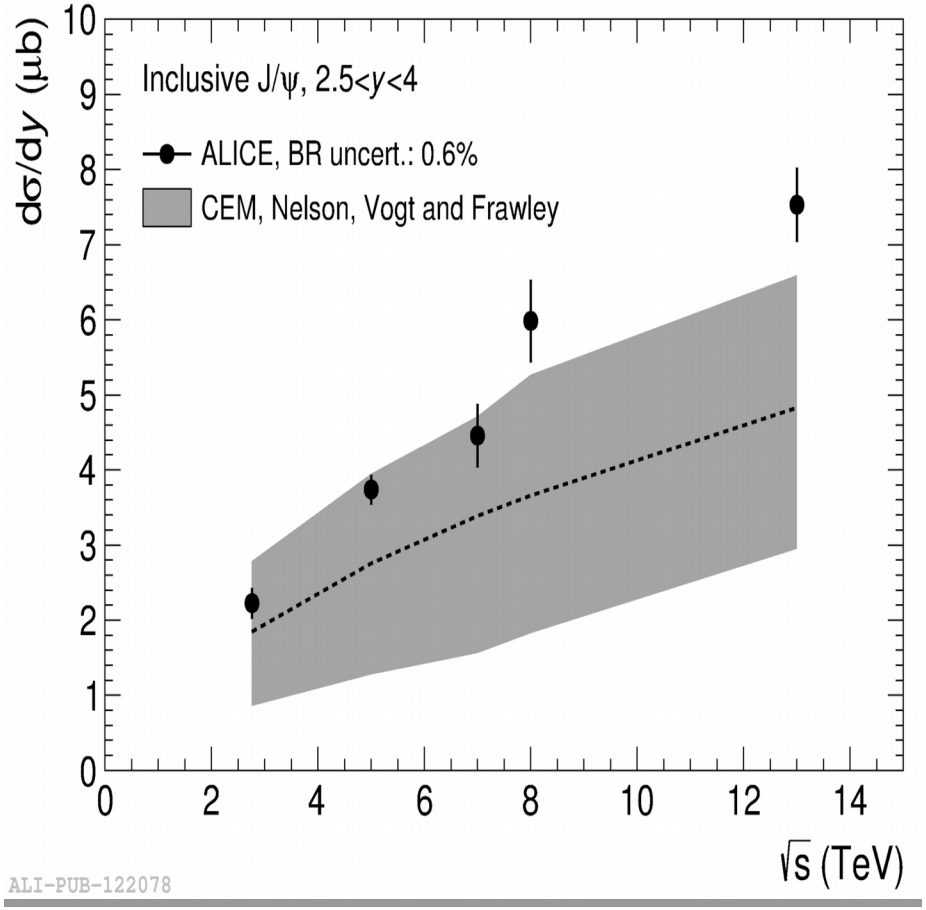

Particle ratio, comparison to NRQCD

Many systematic uncertainties cancel in the particle ratio, for both data and theory

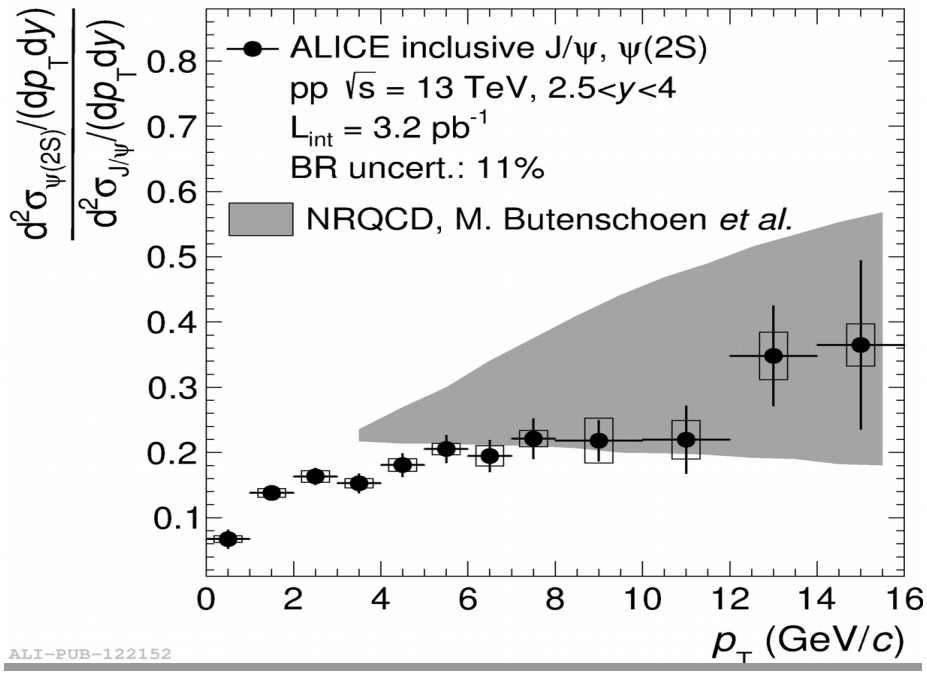

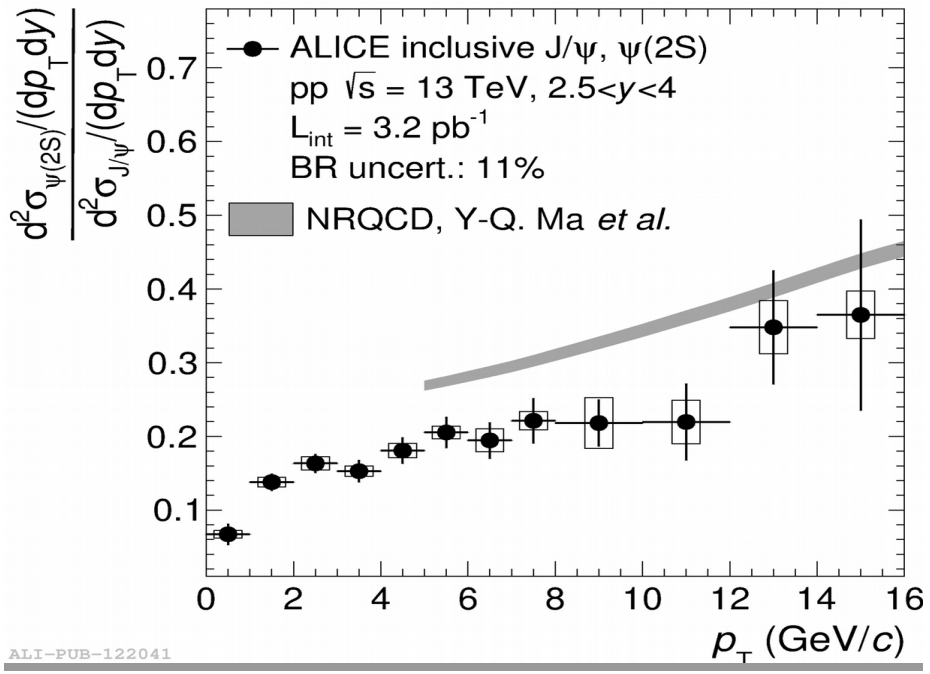

NRQCD (left) Butenschon and Kniel, PRL 106 (2011) 022003
NRQCD (right) Ma, Wang and Chao, PRL 106 (2011) 042002

Both calculations follow the same trend but have very different uncertainties. This was already the case at $\sqrt{s}$ = 7 TeV (see ALICE EPJC 74 (2014) 2974)

Calculation from Y-Q Ma *et al.* tends to overestimate the ψ(2S)-to-J/ψ ratio

Contributions from non-prompt J/ψ and ψ(2S) have little impact here because they enter both the numerator and denominator, with a similar (small) magnitude

Data at all energies vs p_T compared to NRQCD

Extensive data-theory comparisons done at all energies available at the LHC so far.

Good agreement between the model and the data is observed for all measured cross sections, for both

J/ψ and ψ(2S)

For ψ(2S)-to-J/ψ cross section ratios the model tends to be slightly above the data especially at $\sqrt{s}$ =13 TeV.

This tension appears mainly because of the error cancellation between the uncertainties on the J/ψ and ψ(2S) cross sections.

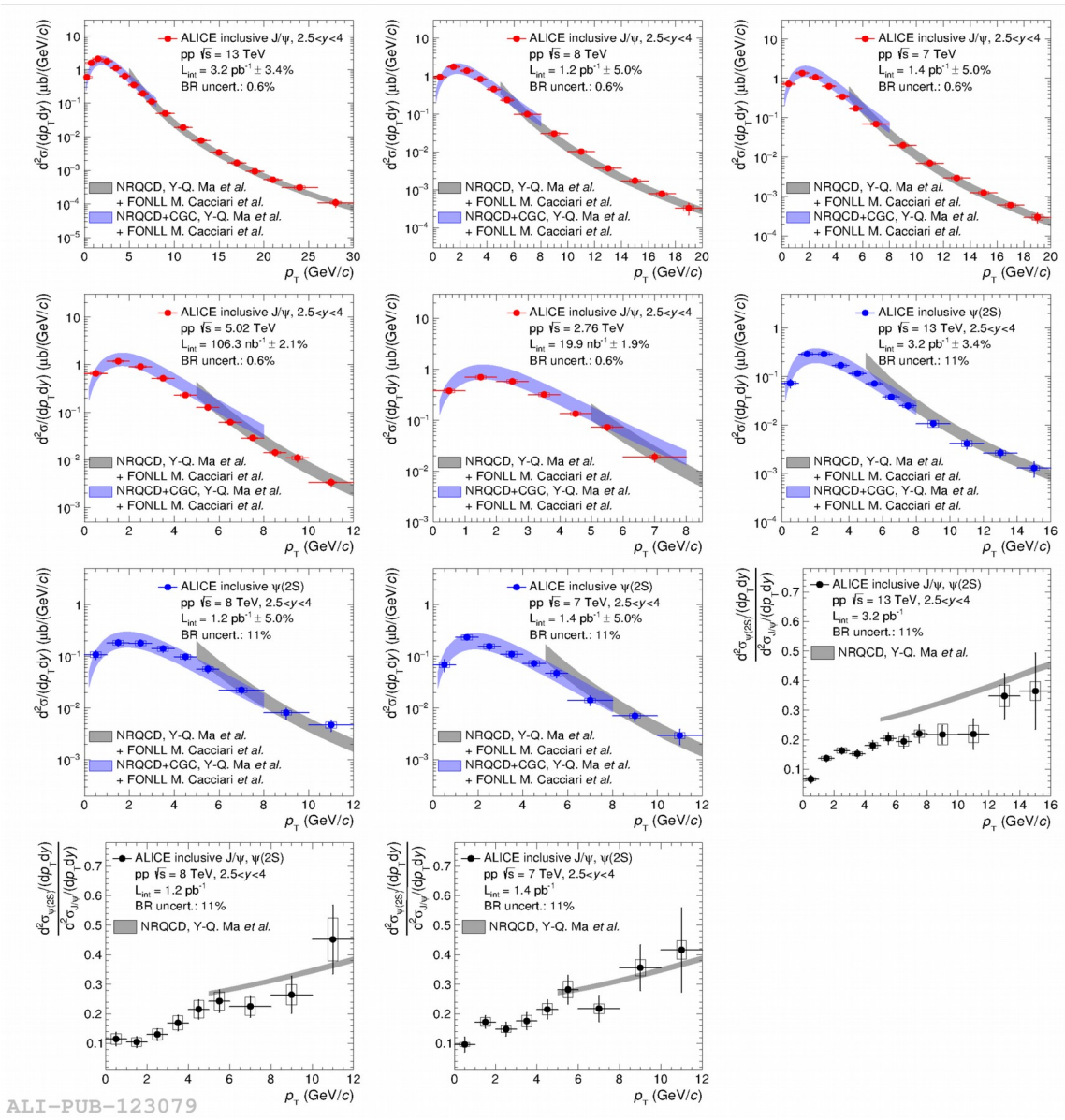

J/ψ polarization and η_c

J/ψ polarization

J/ψ (spin 1) alignment analyzed via the angular distribution of the decay products vs polar (θ) and azimuthal (ϕ) angles:

$$W(\theta,\phi) \propto \frac{1}{3+\lambda_\theta}\left(1+\lambda_\theta \cos^2\theta + \lambda_\phi \sin^2\theta \cos 2\phi + \lambda_{\theta\phi} \sin 2\theta \cos\phi\right)$$

Integrating over ϕ: $$W(\cos\theta) \propto \frac{1}{3+\lambda_\theta}(1+\lambda_\theta \cos^2\theta)$$

Integrating over cosθ: $$W(\phi) \propto 1+\frac{2\lambda_\phi}{3+\lambda_\theta}\cos 2\phi$$

Typically: measure quarkonium corrected yields in bins of cosθ, ϕ and p_T, perform a simultaneous fit using functions above to extract λ_θ and λ_ϕ

J/ψ polarization

J/ψ spin alignment analyzed via the angular distribution of the decay products in the helicity frame

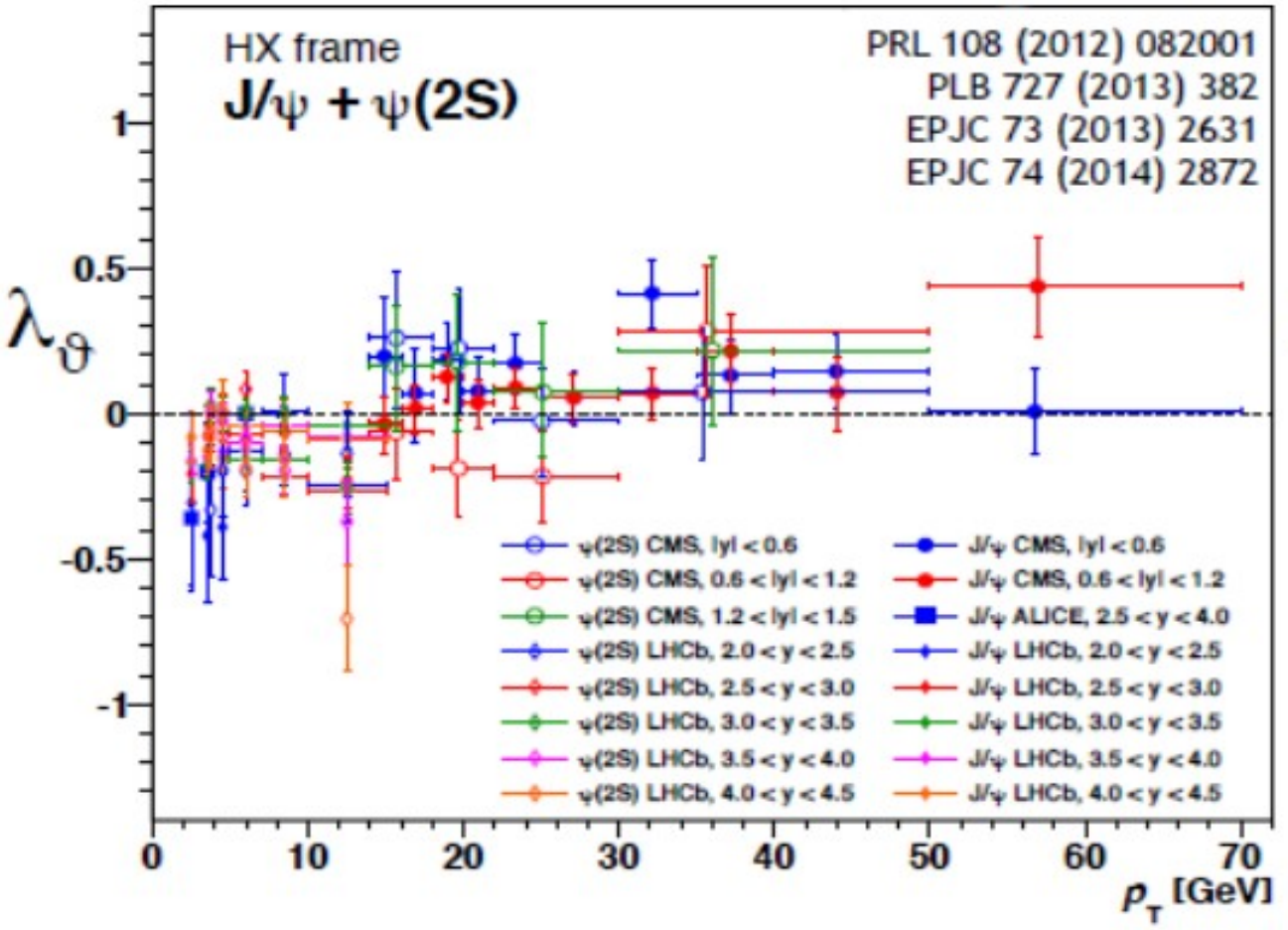

Agreement between CMS, LHCb and ALICE, consistent with zero polarization within the (large) experimental uncertainties

LHCb's η_c measurements

η_c(1S) mesons reconstructed via the ppbar final decay channel.

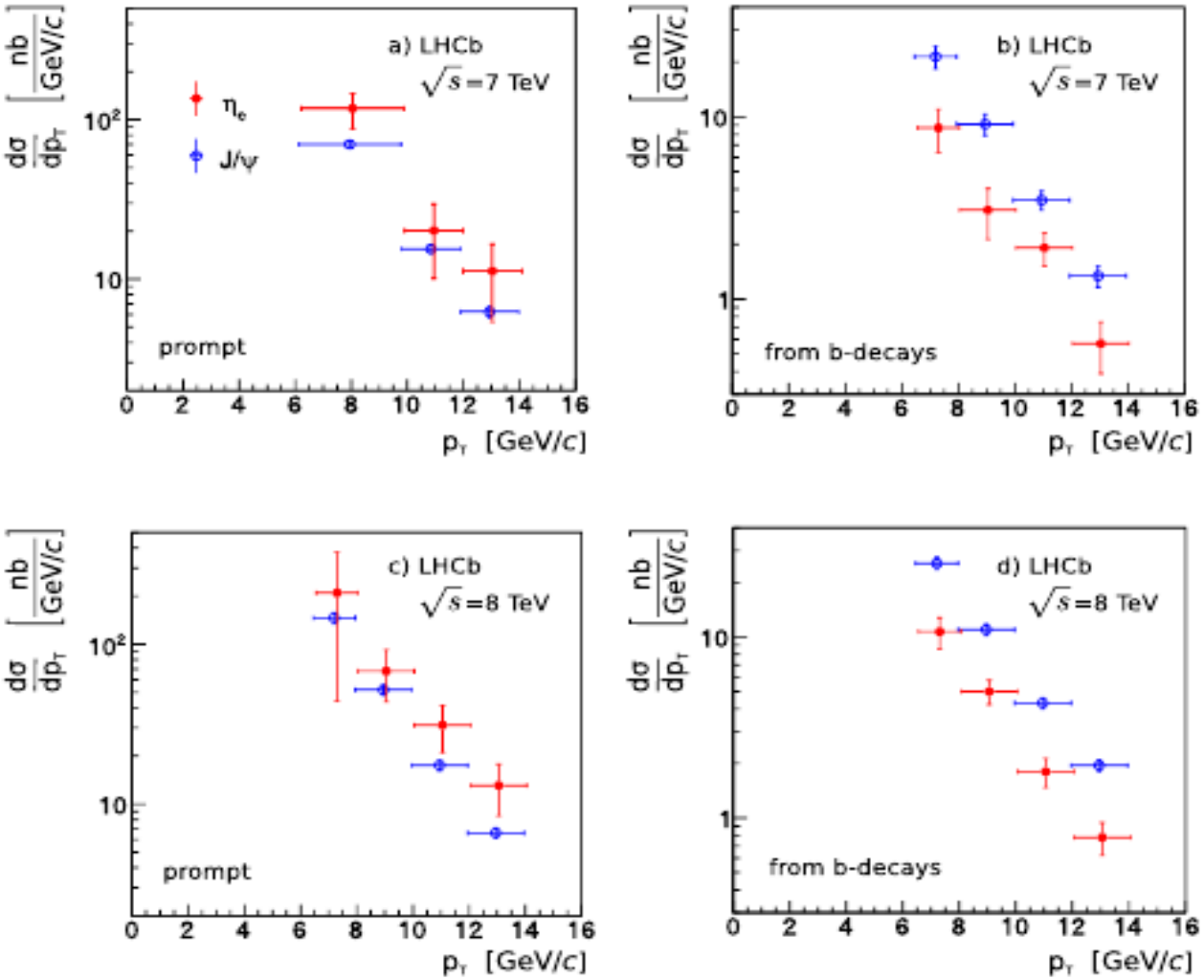

Eur.Phys.J. C75 (2015)

What about model comparisons?

pp yield: **pp polarization:** **ηc production:**

Butenschön, Kniehl:

$\langle O_8^{J/\psi}(^1S_0)\rangle = 0.0497\ \text{GeV}^3$
$\langle O_8^{J/\psi}(^3S_1)\rangle = 0.0022\ \text{GeV}^3$
$\langle O_8^{J/\psi}(^3P_0)\rangle = -0.0161\ \text{GeV}^5$

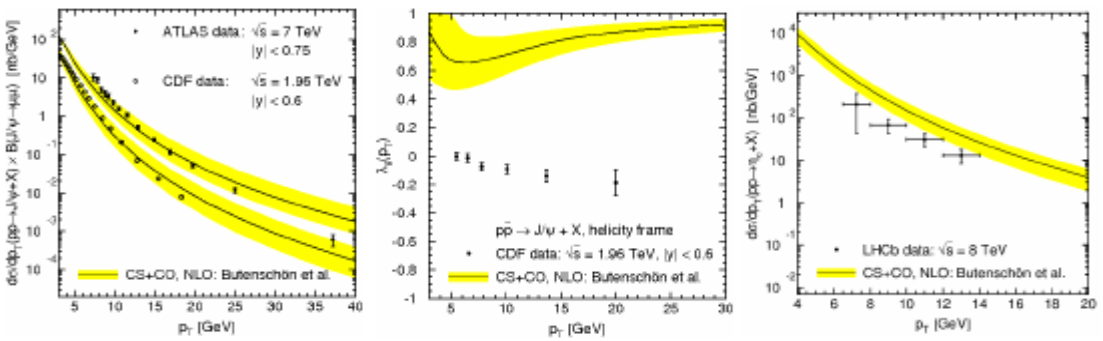

Gong, Wan, J.-X. Wang, H.-F. Zhang:

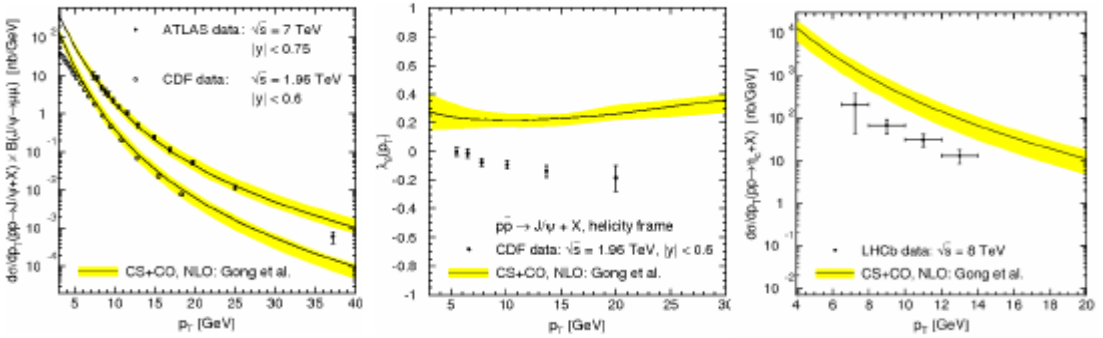

Chao, Ma, Shao, K. Wang, Y.-J. Zhang:

$\langle O_8^{J/\psi}(^1S_0)\rangle = 0.089\ \text{GeV}^3$
$\langle O_8^{J/\psi}(^3S_1)\rangle = 0.003\ \text{GeV}^3$
$\langle O_8^{J/\psi}(^3P_0)\rangle = 0.0126\ \text{GeV}^5$

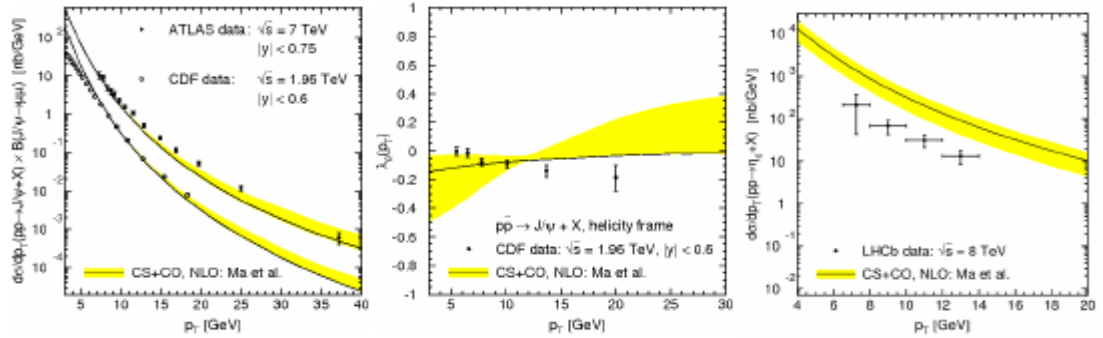

Figure from **KNIEHL B.** Quarkonium 2016 VA, USA

dσ/dy as a function of √s

inclusive J/ψ

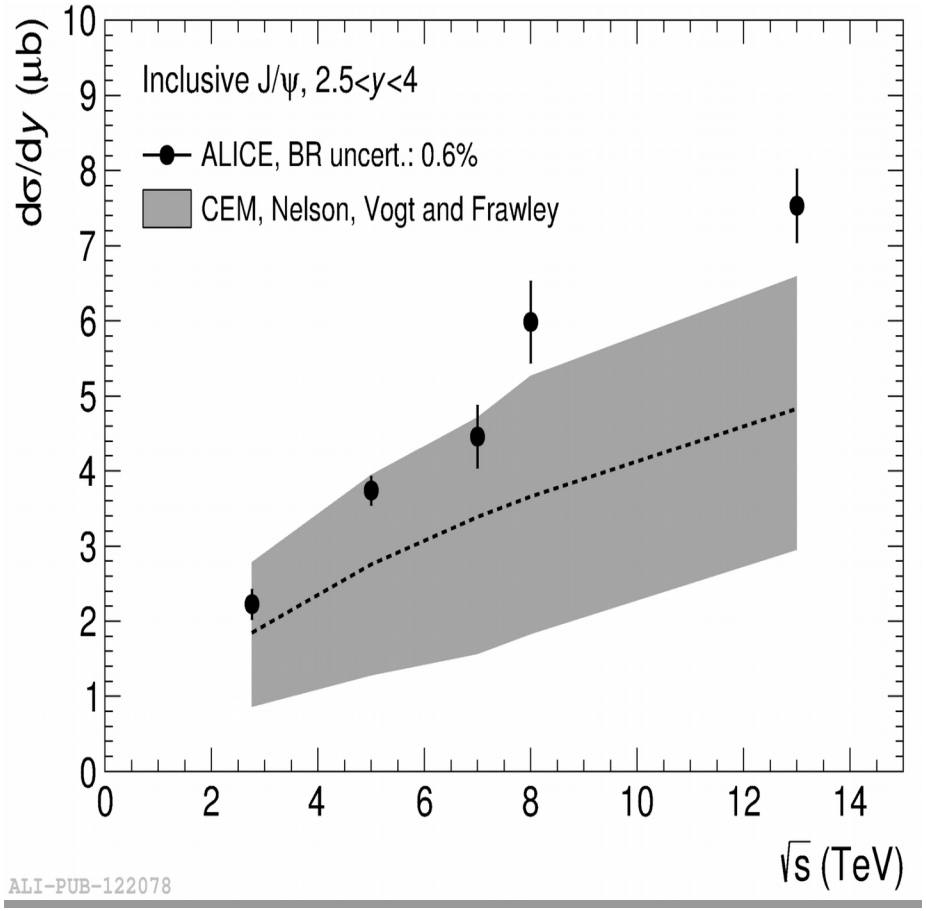

inclusive ψ(2S)

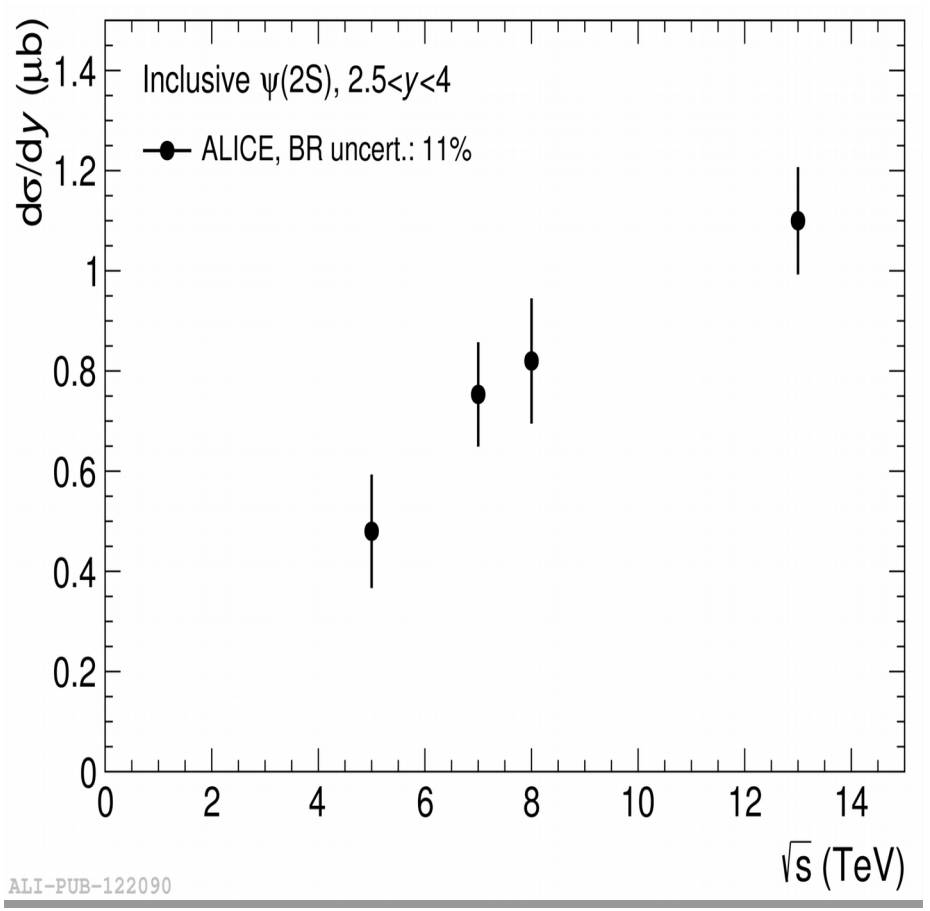

Steady increase of dσ/dy as a function of increasing √s.

For the J/ψ (left), the cross sections are compared to a calculation done by in the CEM framework (PRC 87 014908)

Data lies on the upper side of the calculation and the difference to the central value becomes larger with increasing √s.

Centrality Determination

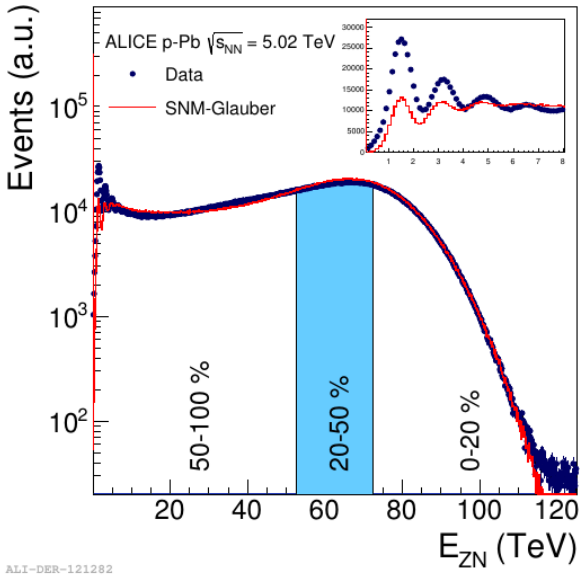

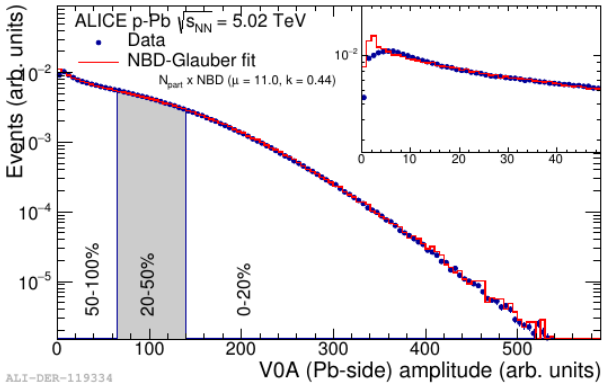

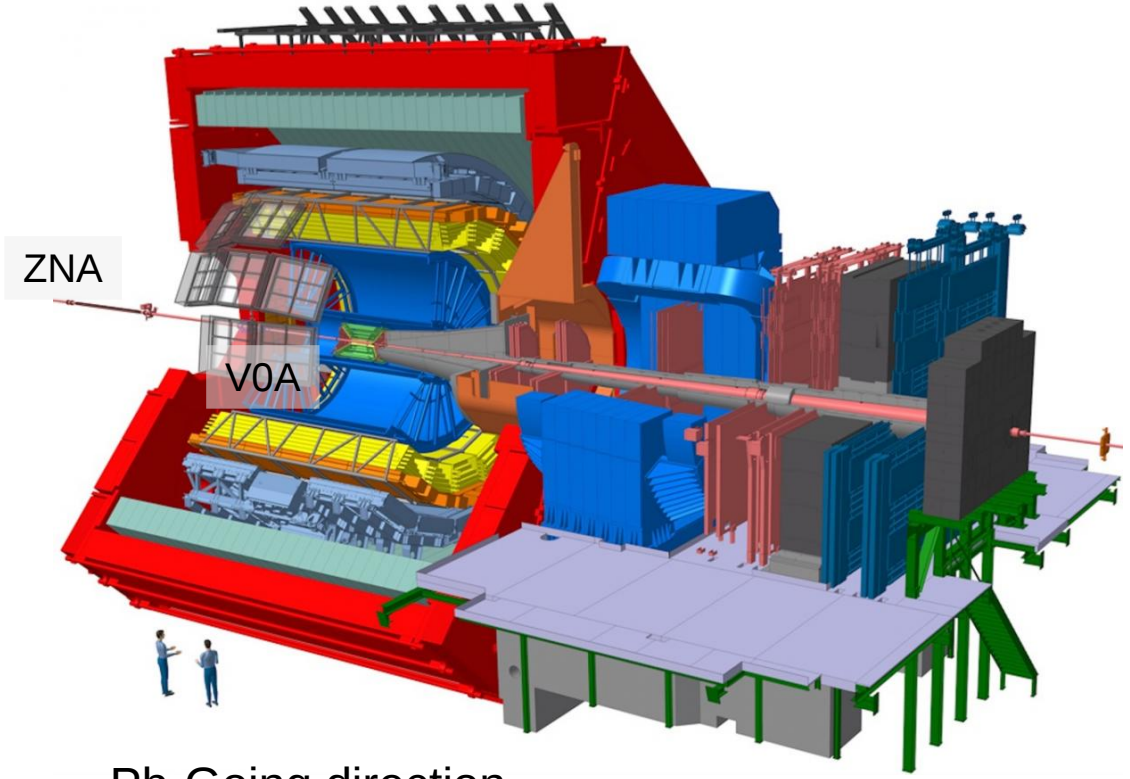

Pb-Going direction

V0 signal is proportional to the number of wounded Pb (target) nucleons s approach assumes that the ($N_{part}^{target} = N_{part} - 1 = N_{coll}$).

The average number of collisions for a given centrality, selected with the ZNA, is then given by scaling the minimum bias value of N_{coll} with the ratio of the average raw signal of the innermost ring of the V0A

ALICE, Phys. Rev. C 91 (2015) 064905

J/ψ production in p-Pb at $\sqrt{s_{NN}}$ = 8.16 TeV

R_{pPb} Double ratio of results $\sqrt{s_{NN}}$ = 8.16 to 5.02 TeV (JHEP 11 (2015) 127)

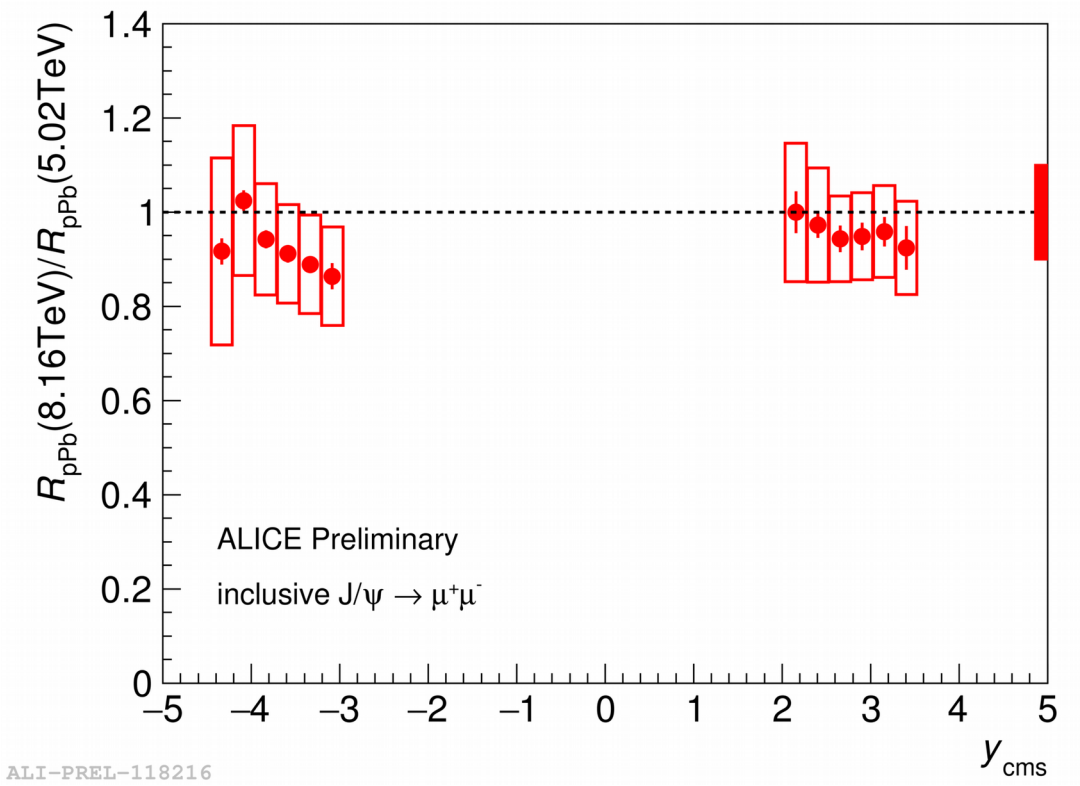

1.1 x10^{-5} < x <5 x10^{-5} (p-going)
7.3 x10^{-3}< x <3.3 x10^{-2} (Pb-going)

Consistent with unity within the experimental errors